Materials Advances

ROYAL SOCIETY OF CHEMISTRY

REVIEW

View Article Online
View Journal | View Issue

Cite this: *Mater. Adv.*, 2026, 7, 1936

Electrochemical cement synthesis: a materials-centered framework for reactor design, manufacturing, and technoeconomic feasibility

Abdallah M. Abdeldaiem and Nageh K. Allam *

The cement industry accounts for approximately 8% of global CO_2 emissions, representing one of the most challenging sectors for decarbonization. Electrochemical approaches to cement synthesis offer a transformative pathway to eliminate process emissions while enabling the utilization of renewable electricity. This comprehensive review critically examines the design principles, operational challenges, and technological advances in electrochemical reactors for cement production. Reactor configurations ranging from three-compartment systems employing bipolar and cation exchange membranes to innovative zero-gap designs, which achieved voltages as low as 0.38 V at 100 mA cm^{-2}, have been analyzed. Key technical challenges including membrane fouling, electrode degradation, and scaling considerations are systematically evaluated alongside emerging solutions such as orthogonalized ion management and composite membrane technologies. Performance metrics demonstrate Faradaic efficiencies approaching 100% with $Ca(OH)_2$ production rates of 486 mg h^{-1}, while techno-economic analyses reveal pathways to cost competitiveness under favorable electricity pricing and carbon policy scenarios. The review identifies critical research priorities including advanced membrane materials, process intensification strategies, and integrated system optimization as essential for commercial deployment. This work provides a foundational framework for understanding the current state and prospects of electrochemical cement synthesis technologies.

Received 22nd November 2025,
Accepted 8th January 2026

DOI: 10.1039/d5ma01359c

rsc.li/materials-advances

Energy Materials Laboratory, School of Sciences & Engineering, The American University in Cairo, New Cairo 11835, Egypt. E-mail: nageh.allam@aucegypt.edu

Abdallah M. Abdeldaiem

Abdallah Abdeldaiem earned his Bsc in Nano Science and Technology with honors from Kafrelsheikh University, Egypt. He currently serves as a Research Assistant at the Energy Materials Laboratory (EML) at The American University in Cairo (AUC). His research focuses on the design of advanced electrolyte systems for high-performance supercapacitors, specifically investigating the physicochemical properties and ionic transport mechanisms of quasi-solid-state hydrogels and deep eutectic solvents. Additionally, he possesses expertise in the synthesis of nanostructured metal oxides and advanced structural characterization for sustainable energy applications.

Nageh K. Allam

Nageh Allam received his PhD in Materials Science and Engineering from Pennsylvania State University. He joined Georgia Institute of Technology as a postdoctoral fellow then Massachusetts Institute of Technology as a Research Scholar. After his postdoctoral tenure, he joined The American University in Cairo, where he is currently a professor of Materials Science and Engineering. His research focuses on the fabrication of well-designed nanostructured materials with composition, size, and shape control for use in energy conversion (Water electrolysis, CO_2 reduction, NH_3 synthesis, Biogas, etc.) and storage (Batteries & Supercapacitors), Capacitive deionization, Electrochemical sensors, Biomaterials, among others. The research comprises both experimental and theoretical activities.

1. Introduction

1.1. The cement industry challenge

The cement industry occupies a unique and critical position in the global economy, producing over 4.5 billion tons of Portland cement annually to serve as the essential binder for concrete, the world's most widely used construction material after water.[1–3] This massive production scale makes cement manufacturing the second-largest industrial contributor to global greenhouse gas emissions, accounting for approximately 8% of worldwide CO_2 emissions and generating an estimated 2.8 billion tons of CO_2 annually.[4–8] To contextualize this environmental impact, if the cement industry were a country, it would rank as the fourth-largest CO_2 emitter globally, surpassing all nations except China, the United States, and India.[9]

The substantial carbon footprint of traditional Portland cement manufacturing, a process that has remained fundamentally unchanged for over 150 years, stems from two primary sources, as illustrated in Fig. 1. The first and most significant source, accounting for approximately 60% of total emissions, is the inherent process chemistry itself: the calcination of limestone (calcium carbonate, $CaCO_3$). In massive, high-temperature rotary kilns operating at 1400–1500 °C, limestone is thermally decomposed into lime (calcium oxide, CaO) and CO_2 at temperatures exceeding 900 °C.[10–13] This chemical reaction ($CaCO_3 \rightarrow CaO + CO_2$) is unavoidable in the conventional thermochemical pathway and inherently releases 0.54 tons of CO_2 for every ton of cement clinker produced.[4,11,14] The second major source, contributing another 30% of emissions, is the combustion of fossil fuels (primarily coal and petroleum coke) required to achieve these extreme process temperatures.[1,2] The remaining 10% of emissions derive from ancillary processes including raw material extraction, transportation, grinding, and facility operations.[15] When including energy-related sources for grinding and transportation, the total emissions typically exceed 0.9 tons of CO_2 per ton of cement.[4,11,14]

The urgency for a fundamental transformation in cement manufacturing has been intensified by converging global trends. Cement demand is projected to increase by 12–23% by 2050, driven by rapid urbanization and infrastructure development in emerging economies.[16–18] This rising demand is in direct conflict with the imperative to achieve deep emissions reductions to meet the goals of the Paris Agreement. The challenge is magnified by the inherent limitations of existing decarbonization strategies. Conventional approaches such as improving energy efficiency, switching to alternative fuels, and implementing end-of-pipe carbon capture and storage (CCS) are crucial but insufficient. Even when fully deployed, these measures can only address an estimated 50–60% of the industry's total emissions, leaving the substantial and unavoidable process emissions from calcination largely unresolved.[16,17,19] This reality underscores the urgent need for a paradigm shift, moving beyond incremental improvements toward transformative technologies that fundamentally reinvent the chemistry of cement production.

1.2. A paradigm shift: electrochemical cement synthesis

A truly transformative pathway is emerging through the electrification of cement synthesis. This approach represents a fundamental paradigm shift that addresses both process and energy emissions simultaneously by replacing high-temperature limestone calcination with ambient-temperature electrochemical processes (Fig. 2a). The concept gained significant momentum following pioneering work by researchers at MIT in 2019, who demonstrated that neutral water electrolysis could be used for limestone decarbonation, achieving near-stoichiometric operation where every two protons generated electrochemically decarbonate one formula unit of $CaCO_3$.[2,22–24] Based on Fig. 2b, the electrochemical production of cement achieves a substantial reduction in carbon emissions, cutting CO_2 output by a minimum of 60% when compared to conventional methods.[21] The fundamental principle behind this process is the strategic exploitation of pH-dependent chemical

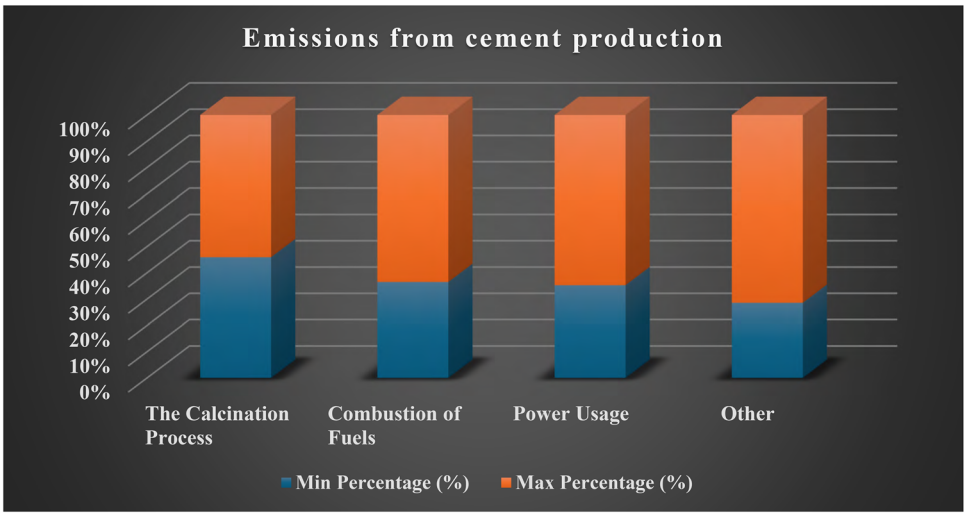

Fig. 1 Schematic breakdown of the primary sources of CO_2 emissions in conventional Portland cement manufacturing. Process emissions from the calcination of limestone are the largest contributor, followed by emissions from the combustion of fossil fuels required to heat the kiln.[2,20,21]

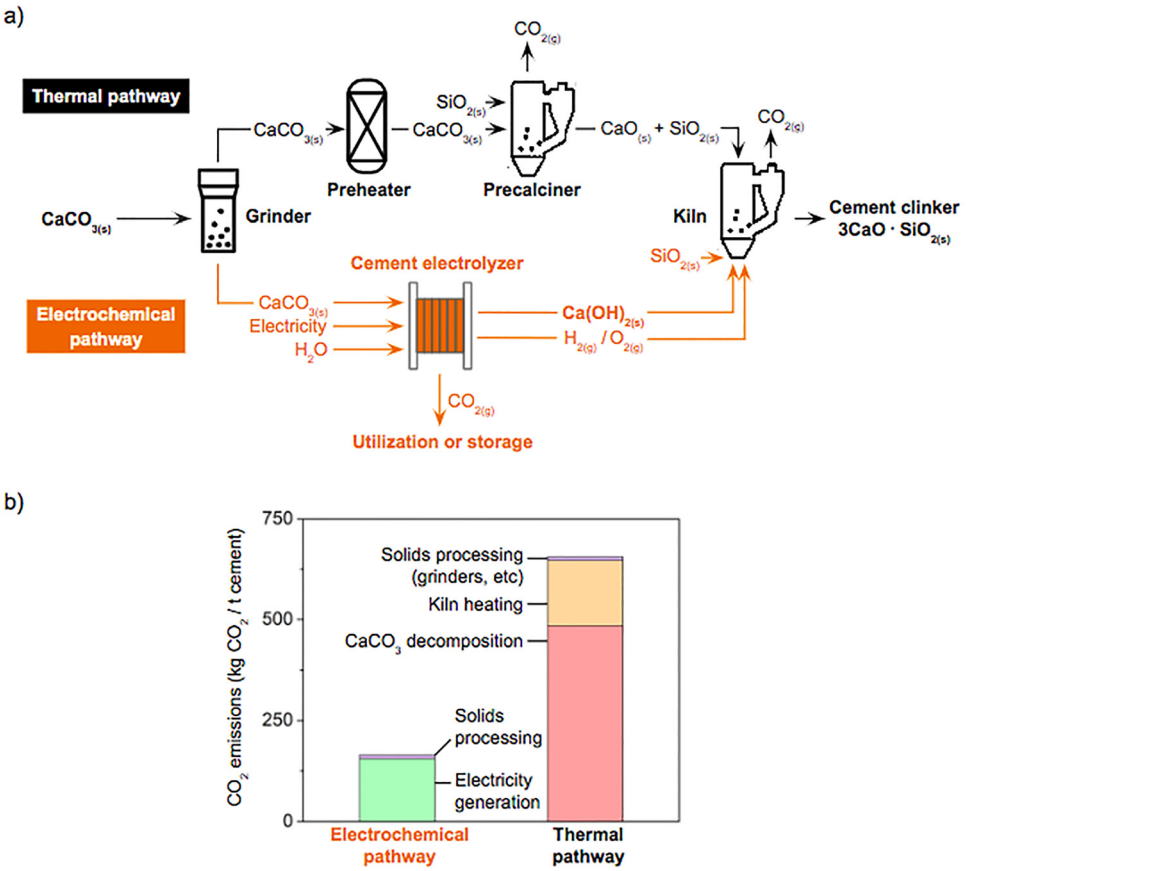

Fig. 2 Comparison of cement production pathways. (a) Schematic contrasting the conventional thermal route (fossil fuel calcination) with the electrochemical route (electrolyzer-based decarbonation yielding pure gas streams and solid precursor). Both pathways conclude with a high-temperature kiln step. (b) Life-cycle assessment (LCA) comparing the CO_2 emissions of both methods. Reprinted with permission from ref. 21. Copyright (2022) the Royal Society of Chemistry.

equilibria, as depicted in Fig. 3. An electrochemical reactor, commonly referred to as an electrolyzer, utilizes electricity to split water (H_2O) causing the liberation of protons (H^+) at the anode and hydroxide ions (OH^-) at the cathode. This establishes a strong pH gradient across the reactor, which drives the desired chemical transformations at ambient temperature:

1. At the anode (low pH): the electrochemically generated protons create a localized acidic environment. In this solution, limestone ($CaCO_3$) readily dissolves into aqueous calcium ions (Ca^{2+}) while releasing its carbon content as a pure stream of gaseous CO_2. This co-product is generated in a concentrated form, making it ideal for direct capture and subsequent utilization or sequestration without the need for energy-intensive separation from flue gases, as is required in conventional plants.[23–25]

$$CaCO_{3(s)} + 2H^+ \rightarrow Ca^{2+} + CO_{2(g)} + H_2O \quad (1)$$

2. At the cathode (high pH): simultaneously, the hydroxide ions create a highly alkaline environment. The Ca^{2+} ions, having migrated from the anode region, react with the abundant hydroxide ions to precipitate as solid calcium hydroxide ($Ca(OH)_2$), also known as portlandite.

$$Ca^{2+} + 2OH^- \rightarrow Ca(OH)_{2(s)} \quad (2)$$

This precipitated $Ca(OH)_2$ serves as a pure, reactive, and fully decarbonated precursor for cement clinker. It can then be processed with silica in a final heating step to form the essential cementitious phases. By powering the electrolyzer with renewable electricity and utilizing the green hydrogen co-produced at the cathode to fuel the final kiln step, the entire manufacturing chain can be rendered virtually emission-free.[22,24] This electrochemical route fundamentally re-engineers the process, capturing carbon at the beginning as a valuable co-product rather than releasing it at the end as a diluted pollutant. Recent developments have demonstrated remarkable performance improvements, with advanced reactor designs achieving cell voltages as low as 0.38 V at 100 mA cm^{-2} and sustained operation for over 50 hours with near-theoretical Faradaic efficiency. These breakthroughs signal a viable pathway toward cost-competitive, zero-emission cement manufacturing.[26,27]

1.3. Thermodynamic and kinetic drivers

The successful implementation of the electrochemical pathway is governed by a set of core physicochemical principles that dictate reactor design and operational efficiency. The process fundamentally replaces the high thermal activation energy of conventional calcination (exceeding 200 kJ mol^{-1}) with

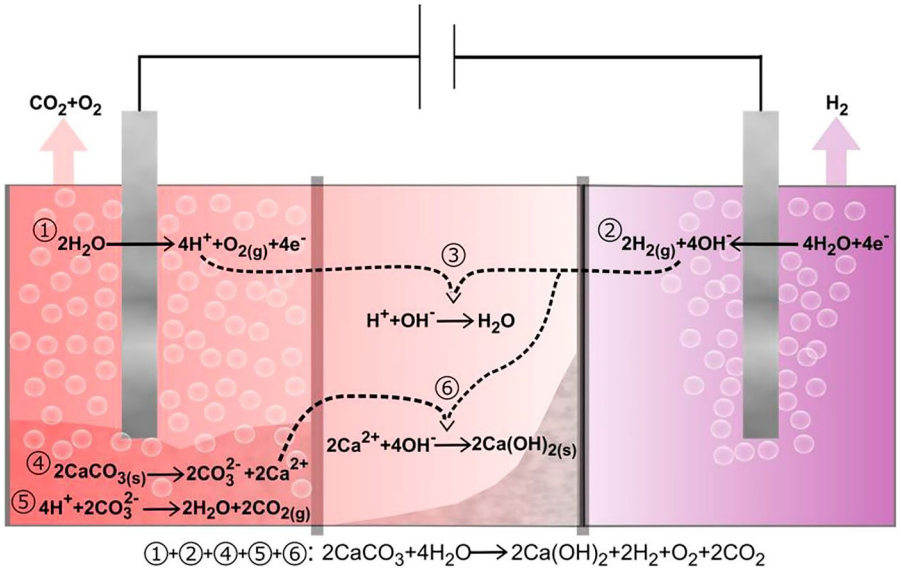

Fig. 3 The fundamental principle of electrochemical cement synthesis. Water electrolysis generates a pH gradient, with protons (H^+) dissolving limestone ($CaCO_3$) at the anode and hydroxide ions (OH^-) precipitating calcium hydroxide ($Ca(OH)_2$) at the cathode. Hydrogen, oxygen, and pure CO_2 are generated as valuable co-products.[24]

catalyzed electrochemical reactions that operate near ambient temperature with relatively low overpotentials.[25,26] The primary thermodynamic driving force stems from the strategic manipulation of pH-dependent equilibrium. The dissolution of limestone is thermodynamically favorable in the acidic environment generated at the anode, with solubility increasing dramatically at pH < 6. Conversely, the precipitation of the desired calcium hydroxide product is favored in the highly alkaline environment of the cathode, occurring readily at pH > 1.25.[25] The creation and maintenance of this steep pH gradient across the reactor is therefore the central operational imperative.

1.4. Reactor design imperatives and technological evolution

The practical and economic viability of electrochemical cement synthesis hinges on the design of the electrochemical reactor. The design of these reactors must address multiple, often competing, objectives. Unlike conventional electrolyzers designed solely for gas production, cement reactors must simultaneously manage a complex multiphase environment involving solid–liquid–gas interfaces, maintain stable pH gradients, and mitigate precipitation phenomena that can hinder performance. The key imperatives include maximizing limestone conversion efficiency, minimizing energy consumption, preventing performance degradation from membrane fouling, and ensuring long-term operational stability, all while producing pure gas streams (H_2, O_2, CO_2) and solid products ($Ca(OH)_2$) suitable for downstream use.[24,26,28]

Reactor technology has evolved from initial batch configurations to continuous flow systems to address scalability requirements. A pivotal development was the multi-compartment flow cell, which spatially isolates anodic, cathodic, and central reactions, thereby enabling the recovery of pure co-product streams.[21] However, membrane fouling (which is characterized by the precipitation of $Ca(OH)_2$ on reactor components) resulted in rapid voltage escalation and system failure.[26] To mitigate this, 'tandem' architectures were introduced to physically decouple electrochemical ion generation from product precipitation. By mixing ion-rich streams in an external vessel, this approach prevents internal fouling and has demonstrated unprecedented long-term operational stability.[26]

1.5. Purpose and scope of this review

This review provides a critical analysis of electrochemical reactor designs for cement synthesis, systematically evaluating reactor configurations, technological advances, operational challenges, and commercialization prospects. By examining fundamental principles and key performance metrics, this work establishes a framework for understanding the current state of the technology and identifies critical research priorities and engineering challenges needed to accelerate deployment of electrochemical cement synthesis.

2. Electrochemical reactor configurations

Since the initial proof-of-concept, research has diversified into several distinct reactor architectures, each aiming to address specific challenges related to efficiency, durability, and scalability. It is also important to distinguish the operational modes employed across the following studies. For instance, Ellis *et al.*[24] primarily utilized potentiostatic control to characterize fundamental reaction kinetics and thermodynamic feasibility. In contrast, subsequent scale-up efforts (*e.g.*, Zhang *et al.*,[21] Xu *et al.*,[29] and Mowbray *et al.*[30]) shifted to galvanostatic operation to define stable production rates and evaluate

energy efficiency under conditions representative of industrial compliance.

2.1. pH-modulated two-chamber systems

Ellis *et al.*[24] developed a pioneering two-chamber H-cell design using platinum electrodes separated by a porous barrier rather than complex ion-exchange membranes. In this configuration, precise electrolyte selection (chemically inert 1 M $NaNO_3$ or $NaClO_4$) allows for the establishment of steep pH gradients essential for operation. A critical engineering challenge identified in this layout was the management of fluid dynamics; without a physical separator, density-driven currents and gas bubble turbulence caused convective mixing of the acidic anolyte and alkaline catholyte. This mixing led to uncontrolled $Ca(OH)_2$ precipitation directly on the cathode surface, resulting in immediate passivation. By incorporating a porous paper separator to enforce a diffusion-dominated transport regime, the system operated stably at an applied potential of 3.5 V, achieving a Faradaic efficiency of ~85%. This demonstrated that an electrochemical pH gradient could effectively drive the decarbonation of $CaCO_3$ to yield high-purity (94%) $Ca(OH)_2$ suitable for clinker production (as shown in Fig. 4).

Xu *et al.*[29] introduced dynamic electrolyte engineering to resolve the persistent trade-off between limestone dissolution and membrane fouling (Fig. 5). To manage anode stability, they implemented intermittent stirring, creating a "self-cleaning" cycle: while stirring facilitated decarbonization at pH ≈ 5.1, pausing it allowed localized proton accumulation (pH ≈ 1) to dissolve nascent calcium scales. The most significant advance, however, addressed cathode-side fouling. The authors demonstrated that a standard $NaNO_3$ catholyte creates an extreme interfacial pH of 12.4, causing rapid precipitation and

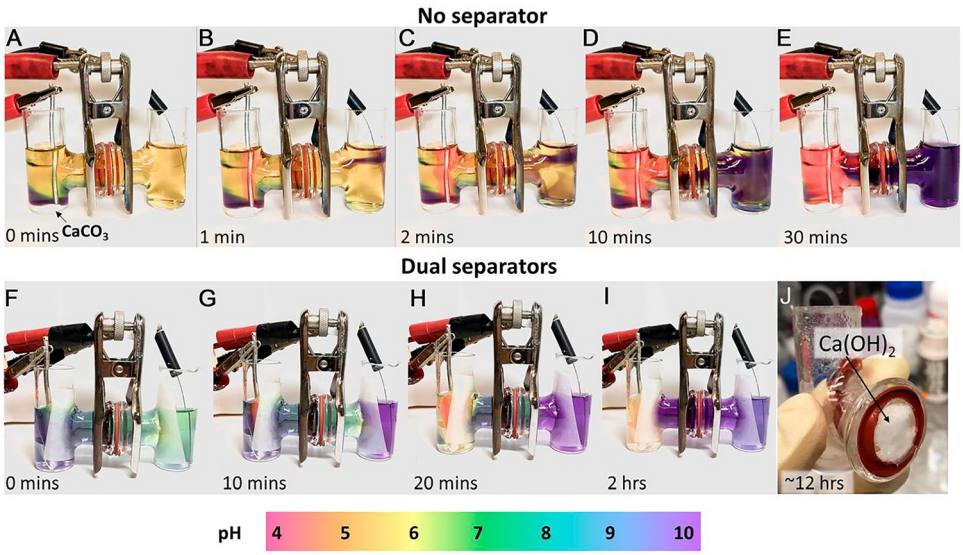

Fig. 4 Time-lapse comparison of H-cell reactor configurations for electrochemical decarbonation (electrolyte: 1 M $NaNO_3$ with pH indicator). (A)–(E) Separator-free configuration: applying 2.5 V (generating an approximate total current of 6 mA) establishes a pH gradient but results in distinct solution stratification in the connecting tube due to density-driven convection. (F)–(I) Configuration with porous separators: the separators physically confine convective mixing, eliminating stratification and maintaining stable pH zones. (J) Solid $Ca(OH)_2$ precipitate formed in the connecting tube after 12 hours of operation.[24]

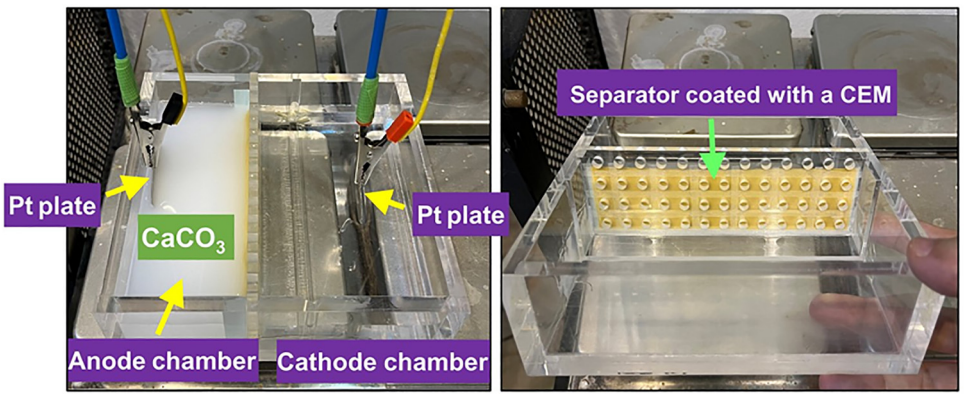

Fig. 5 Image depicting an H-cell electrolyzer (14 cm^3) configured for the electrochemical synthesis of cement clinker precursors.[29]

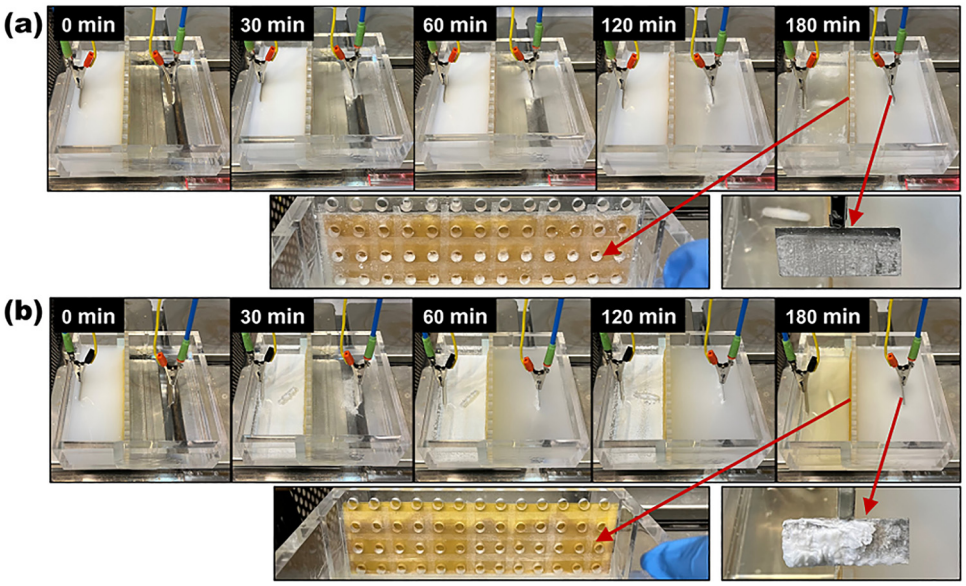

Fig. 6 A sequence of images captured over time shows the formation of $Ca(OH)_2$ during the electrolysis process within a cement clinker precursor reactor. The deposition patterns of the $Ca(OH)_2$ product on the electrode and membrane are displayed after 3 hours for two different catholyte conditions: (a) an initial catholyte with no calcium ions and (b) one containing 0.2 M Ca^{2+}.[29]

membrane blockage (Fig. 6a), limiting Faradaic efficiency to 59%. By pre-doping the catholyte with 0.2 M $Ca(NO_3)_2$, they successfully shifted the precipitation zone from the membrane surface to the bulk solution (Fig. 6b). This reduced the interfacial pH to 11.8, effectively eliminating fouling and boosting the $Ca(OH)_2$ production efficiency to a record 84% at 180 mA cm^{-2} (1150 mg h^{-1}).

Ramírez-Amaya *et al.*[31] applied the H-cell framework to genuine, low-grade limestone feedstocks (68–84% $CaCO_3$). Operating at 9.0 V with a simple filter paper separator (Fig. 7), the process proved remarkably resilient to impurities, showing no significant performance penalty compared to high-purity controls. Crucially, the system demonstrated an intrinsic upgrading capability: the electrochemical dissolution–precipitation cycle selectively concentrated calcium while rejecting contaminants like silica and alumina, yielding a $Ca(OH)_2$ product purer than the original raw material. Although the total calcium recovery in this batch configuration was modest (<30%), these results confirm that electrochemical decarbonation can effectively process and purify the heterogeneous feedstocks characteristic of cement manufacturing.

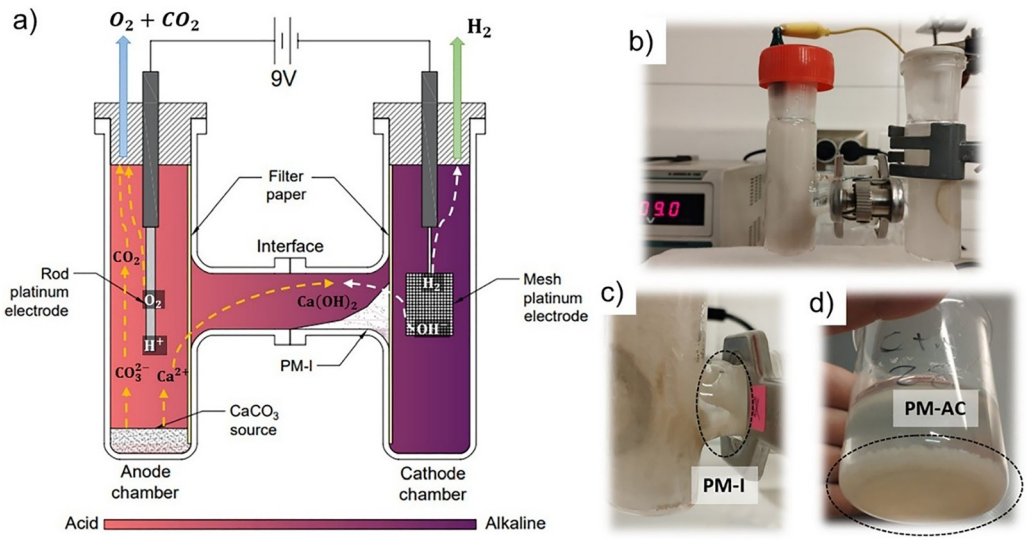

Fig. 7 Depicted are the electrochemical decarbonation (ED) process concept (a), its experimental apparatus (b), the location where precipitated material (PM) forms within the cell (c), and the PM obtained after combining the anode and cathode chamber solutions (d). Reprinted with permission from ref. 31. Copyright (2023) Elsevier.

2.2. Three-compartment flow systems

Zhang *et al.*[21] developed a modular three-compartment flow electrolyzer (Fig. 8). This architecture isolates the anodic, central, and cathodic processes using a bipolar membrane (BPM) to supply protons for limestone dissolution and a cation exchange membrane (CEM) to selectively transport Ca^{2+} for precipitation. Operating with cost-effective nickel foam electrodes and circulating electrolytes (1.0 M KOH anolyte, $CaCO_3$ slurry, and 1.0 M KCl catholyte), the system achieved near-perfect Faradaic efficiency (~100%) at an industrially relevant current density of 100 mA cm^{-2}. This configuration yielded 486 mg h^{-1} of $Ca(OH)_2$ at a cell voltage of 2.9 V while simultaneously producing three high-purity gas streams (O_2, CO_2, and H_2). Despite these advantages, the study identified a critical durability challenge: the gradual accumulation of solid $Ca(OH)_2$ on the CEM surface led to progressive voltage increases, underscoring the necessity for advanced fouling mitigation strategies in continuously fed systems.

2.3. Low-voltage electrolyzer configurations

Mowbray *et al.*[30] re-engineered the three-chamber electrolyzer by implementing a hydrogen oxidation reaction (HOR) anode. The reactor hardware was additively manufactured, featuring a modular design with separate anode, chemical, and cathode chambers secured by aluminum compression plates, as detailed in the exploded and assembled views in Fig. 10a and b. This configuration replaced the high-overpotential bipolar membrane with a low-resistance CEM (Nafion 211) and utilized a Pt/C gas diffusion electrode fed with humidified hydrogen (Fig. 9).

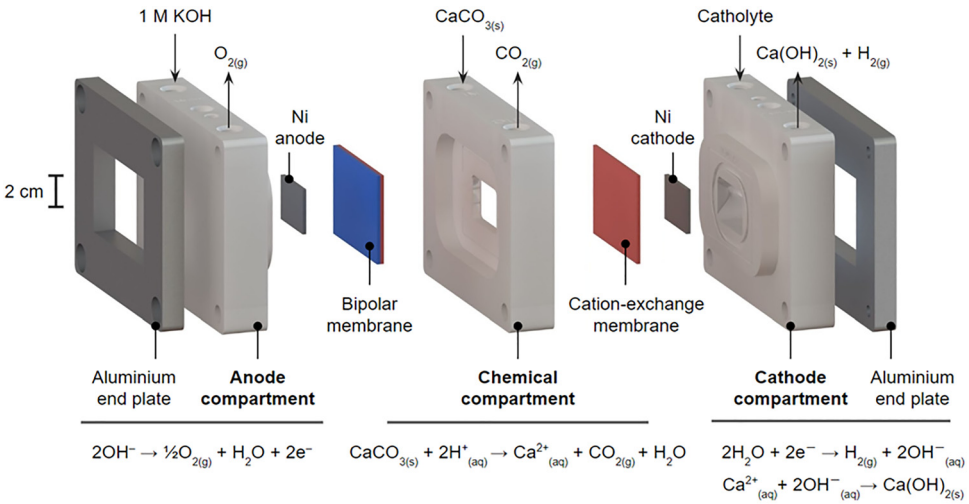

Fig. 8 Schematic of the three-compartment flow electrolyzer for continuous cement precursor production. The system isolates the anode, central (chemical), and cathode chambers using a BPM and a CEM, respectively. Nickel foam electrodes are employed for both the anode and cathode, with balanced equations illustrating the specific reactions in each compartment. Reprinted with permission from ref. 21. Copyright (2022) the Royal Society of Chemistry.

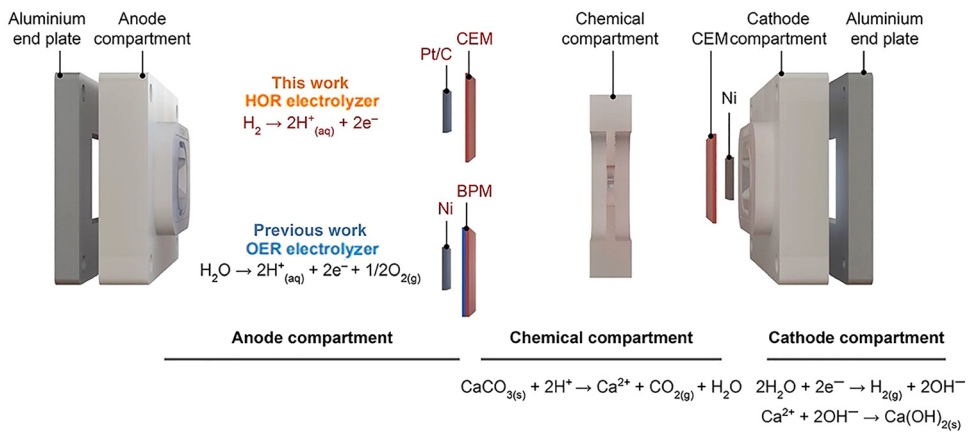

Fig. 9 Schematic comparison of the HOR and OER three-chamber electrolyzer configurations. The HOR system utilizes two CEMs with a platinum-based gas diffusion anode and nickel foam cathode. The OER system employs a BPM adjacent to the anode and a CEM adjacent to the cathode, using nickel foam for both electrodes. Stoichiometrically balanced reactions are provided for each compartment. Reprinted with permission from ref. 30. Copyright (2023) American Chemical Society.

Crucially, this architecture enables the H_2 evolved at the cathode to be recirculated to the anode, creating a cycle that drastically lowers the energy barrier. Operating at 100 mA cm^{-2}, the reactor achieved a remarkably low cell voltage of 1.77 V, which is less than half the 4.2 V required by the OER baseline. However, this energetic gain involved a trade-off: Faradaic efficiency dropped to 70–90% (compared to ~100% for OER systems), attributed to parasitic proton migration across the dual-CEM stack directly to the cathode.

2.4. Tandem (Cascade) reactor systems

Zhang *et al.*[26] addressed persistent membrane fouling by physically decoupling electrochemical ion generation from chemical precipitation. The system utilizes a three-compartment electrolyzer featuring a novel polyaniline (PANI)-coated Nafion cation exchange membrane (CEM) designed for high monovalent cation selectivity. This configuration introduces ''orthogonalized ion vectors'', where K^+ replaces Ca^{2+} as the primary charge carrier across the CEM. Consequently, the electrolyzer generates separate Ca^{2+}-rich and OH^--rich streams that are mixed in an external reactor to precipitate $Ca(OH)_2$ (Fig. 11). By isolating the solid product from sensitive reactor components, this design achieved unprecedented stability, maintaining a cell voltage of ~5 V for 50 hours at 100 mA cm^{-2}, and was successfully scaled to a 100 cm^2 zero-gap system.

Miao *et al.*[32] introduced anion-mediated electrochemical calcium extraction (ECE), a multi-stage process separating limestone dissolution from electrolysis. First, solid $CaCO_3$ is neutralized with a regenerable HCl/HOCl blend (Fig. 12), releasing pure gaseous CO_2 and generating a soluble calcium electrolyte. This solution feeds a custom three-chamber electrolyzer featuring a dual-membrane configuration (CEM and AEM) with an IrO_2 anode and Pt/C cathode (Fig. 13). During operation, anodic chlorine evolution (ClER) and cathodic hydrogen evolution (HER) drive the migration of Ca^{2+} and OH^- into the central chamber, where $Ca(OH)_2$ precipitates. To prevent membrane scaling at high current densities (200 mA cm^{-2}), the design incorporates a continuous NaCl flush and an *in operando* mechanical wiper. The system achieved 93% faradaic yield at ~2.8 V with stability exceeding 13 hours. The platform also demonstrated versatility by processing carbon-free gypsum ($CaSO_4$) *via* anodic oxygen evolution, yielding high-purity $Ca(OH)_2$ at 3.4 V.

Ji *et al.*[33] developed a multi-stage ''cement recycler'' to electrochemically recover constituents from cement waste (Fig. 14). The tandem system uses three interconnected modules: a central acid/base-producing electrolyzer, an external calcium extractor for waste digestion, and a lime extractor for product recovery. This modular design isolates the aggressive chemical digestion from the electrochemical components to improve durability. The core electrolyzer is a three-chamber, OER-based flow cell with nickel foam electrodes, a bipolar membrane BPM, and CEM.

The process operates *via* a recirculating electrolyte loop containing 0.2 M $CaCl_2$ and 1 M KCl. The BPM acidifies the electrolyte to a pH of 0.5–1.0, which is then routed to the calcium extractor to dissolve Ca^{2+} from pulverized cement waste, leaving a purified silica (SiO_2) residue. The Ca^{2+}-rich solution returns to the electrolyzer's cathode, where it reacts with electrogenerated OH^- to precipitate $Ca(OH)_2$. The solid product is filtered out in the lime extractor, and the clarified electrolyte is recycled. The system effectively processed both new and aged cement waste at current densities up to 300 mA cm^{-2}, achieving >80% $Ca(OH)_2$ yields and >90% purity. This recycling method reduced CO_2 output by 99.8% for fresh waste and 80% for aged, carbonated cement. Stable operation was demonstrated for 15 hours, and minor voltage drift from membrane fouling was reversible with inline HCl cleaning, establishing a viable pathway toward cement circularity.

2.5. Zero-gap electrolyzer innovation

Ji *et al.*[27] reconfigured the reactor into an integrated two-chamber, zero-gap flow cell to minimize ohmic losses (Fig. 15). This design

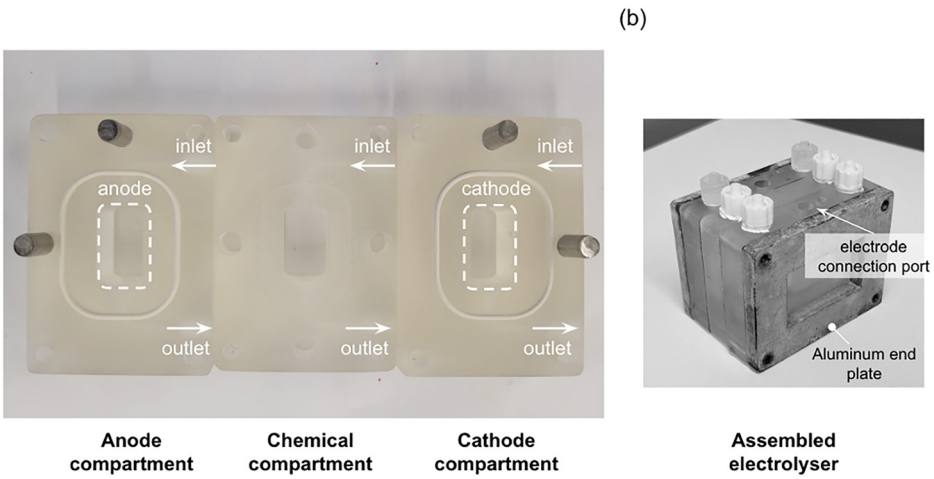

Fig. 10 Images of an additively manufactured three-chamber electrolyzer for cement production. (a) Exploded view showing the separate anode, chemical reaction, and cathode chambers. (b) The fully assembled cell secured with aluminum compression plates. Reprinted with permission from ref. 30. Copyright (2023) American Chemical Society.

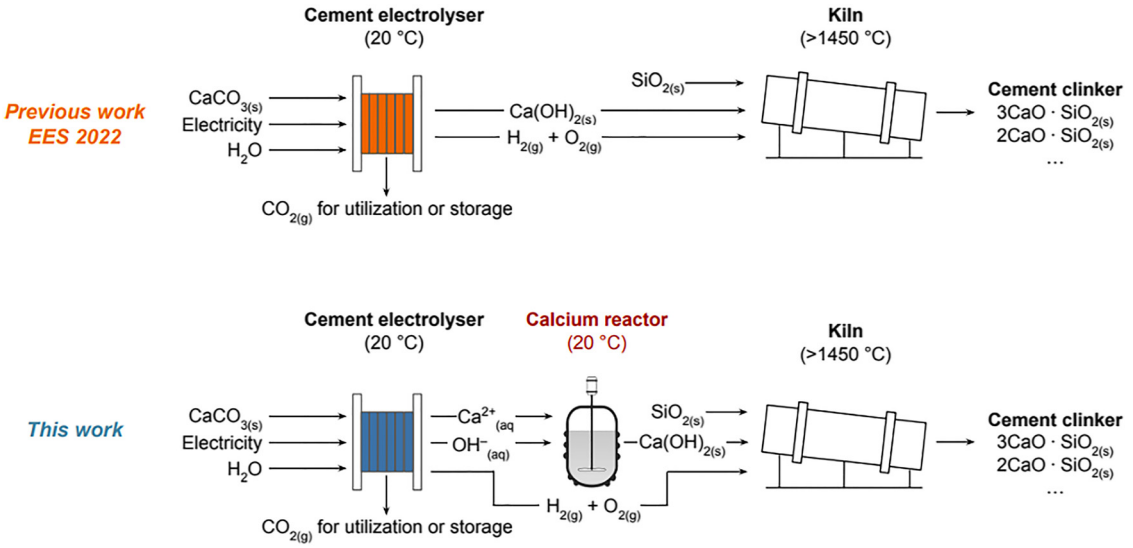

Fig. 11 Comparison of electrochemical cement production pathways. Top: direct *in situ* $Ca(OH)_2$ synthesis within the electrolyzer. Bottom: tandem approach decoupling electrochemical ion generation from *ex situ* precipitation in a separate reactor. Both routes produce $Ca(OH)_2$ precursors for subsequent clinker formation. Reprinted with permission from ref. 26. Copyright (2025) the Royal Society of Chemistry.

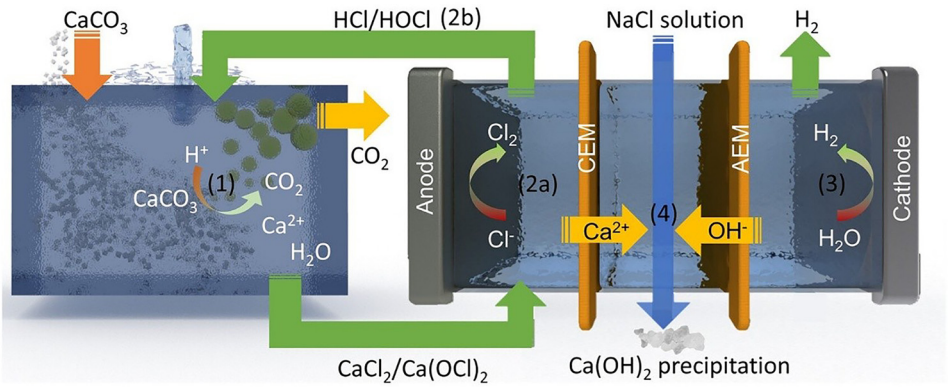

Fig. 12 A diagram of the electrochemical calcium extraction (ECE) method for producing calcium hydroxide ($Ca(OH)_2$). Reprinted with permission from ref. 32. Copyright (2023) American Chemical Society.

eliminates the central chamber, utilizing a single polyaniline-functionalized cation exchange membrane (PANI-CEM) to block Ca^{2+} crossover. The system relies on a proton-coupled electron transfer (PCET) cycle mediated by 9,10-anthraquinone-2,7-disulphonic acid (AQDS). As indicated in Fig. 16, this molecule comprises a rigid anthraquinone core functionalized with sulfonate groups at the 2,7-positions to ensure aqueous solubility. Oxidation of the reduced form (H_2AQ) at the anode releases protons for the direct dissolution of limestone suspended in the anolyte. While initial aqueous tests achieved 1.3 V at 100 mA cm^{-2}, adopting a mixed-solvent electrolyte (4 : 1 water:acetonitrile) at 60 °C suppressed quinone dimer byproduct formation and lowered the cell voltage to an unprecedented 0.38 V, sustaining operation at 4.23 V under an extreme current density of 1 A cm^{-2}, all while maintaining 100% Faradaic efficiency.

The organic solvent modifies the solvation environment, shifting the pK_a values of the H_2AQ acidic protons higher than their standard aqueous values of ~7.6 and 10.6 (±0.2).[34] This shift allows the catholyte to reach a pH of 13.2, surpassing the thermodynamic limit of ~11.8 in pure water, thereby enhancing the driving force for $Ca(OH)_2$ precipitation. Despite these efficiency gains, the inclusion of acetonitrile introduces distinct technoeconomic and environmental challenges regarding solvent management. Although the process utilizes closed-loop recycling, experimental data indicates a volumetric electrolyte loss of ~3% per cycle.[27] Recovery is complicated by the formation of a water-acetonitrile azeotrope, which typically requires energy-intensive pressure-swing or extractive distillation to resolve, adding significant capital and operational costs.[35] Furthermore, because acetonitrile is a volatile organic compound, rigorous recovery is mandatory to meet environmental safety standards and offset rising solvent market prices.[36] Table 1 summarizes the trade-offs between cell voltage, Faradaic efficiency, and complexity across these evolving reactor configurations.

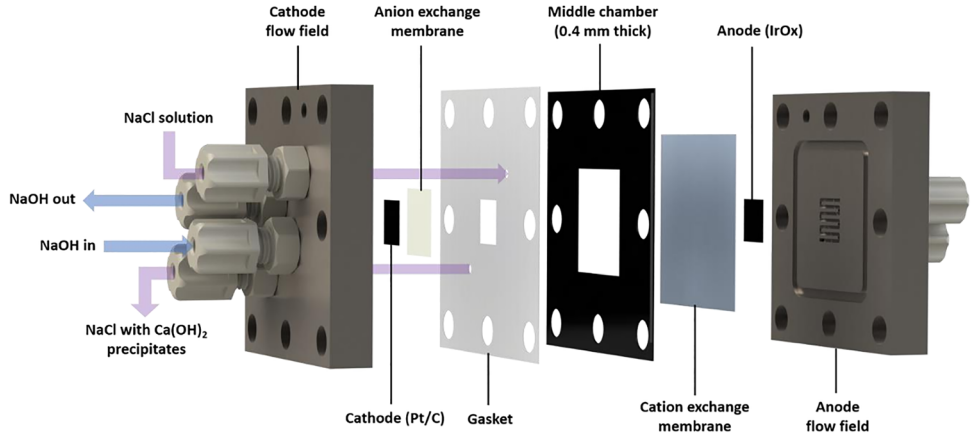

Fig. 13 Expanded view of the electrolyzer assembly employed for the anion-mediated ECE process depicted in Fig. 12. The diagram details the arrangement of the specific components, including the IrO_2 anode, Pt/C cathode, and the dual-membrane stack (CEM and AEM). Reprinted with permission from ref. 32. Copyright (2023) American Chemical Society.

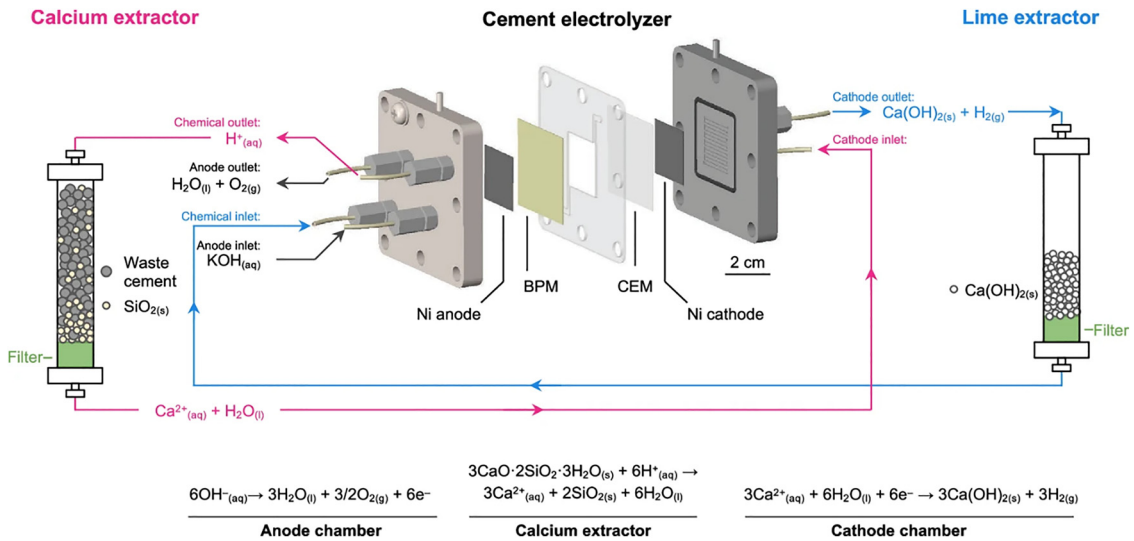

Fig. 14 System layout of the 'cement recycler' system coupling a central electrolyzer with external calcium and lime extractors. Protons generated by the bipolar membrane acidify the recirculating electrolyte (0.2 M $CaCl_2$/1 M KCl) to dissolve calcium from waste cement. The resulting Ca^{2+}-rich stream enters the cathode chamber to precipitate $Ca(OH)_2$, which is harvested in the lime extractor. A separate 3 M KOH loop supports the anode. Reprinted with permission from ref. 33.

3. Membrane technologies and fouling mitigation

Electrochemical cement reactor performance relies on ion exchange membranes to maintain pH gradients and govern selective ion transport.[21,24,29] While these polymer films prevent reactant mixing, the aggressive acidic/alkaline environments and supersaturated species make them susceptible to failure. Consequently, membrane fouling and degradation remain the primary barriers to long-term industrial deployment.[24,28,29,37]

3.1. Bipolar membrane design and function

Bipolar membranes (BPMs) drive pH gradient generation in three-compartment architectures.[21,26] Comprising laminated cation (CEL) and anion exchange layers (AEL), BPMs under reverse bias catalytically dissociate water into continuous H^+ and OH^- fluxes.[21,38–41] In cement electrolyzers, the BPM delivers protons for limestone acid-leaching and hydroxide ions for the anodic oxygen evolution reaction (OER).[21] While BPMs enable salt-free acid/base generation, they incur significant energy penalties. The thermodynamic potential for water dissociation (0.83 V) combined with practical overpotentials results in voltage drops often exceeding 1 V.[30,43] This contributes significantly to the high cell voltages (2.9–4.2 V) in conventional OER-based systems, necessitating efficiency improvements or alternative reactor designs.[21,27,30]

3.2. Cation exchange membrane fouling and degradation

Cation exchange membranes (CEMs), typically perfluorosulfonic acid (PFSA)-based ones (*e.g.*, Nafion), separate the central

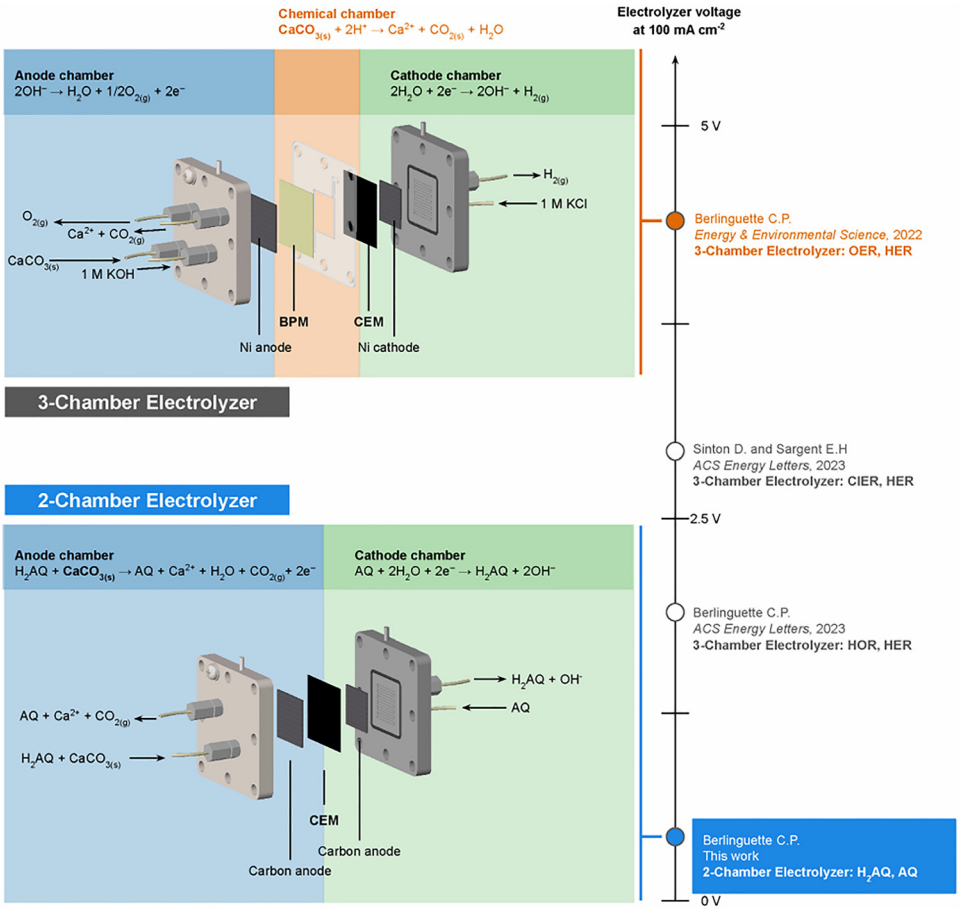

Fig. 15 Operating voltage comparison at 100 mA cm^{-2} for 3-chamber and 2-chamber cement electrolyzers. A schematic illustrates reactor configurations and key electrochemical reactions: hydrogen oxidation (HOR), chloride oxidation (ClER), hydrogen evolution (HER), and oxygen evolution (OER). Reprinted with permission from ref. 27. Copyright (2025) American Chemical Society.

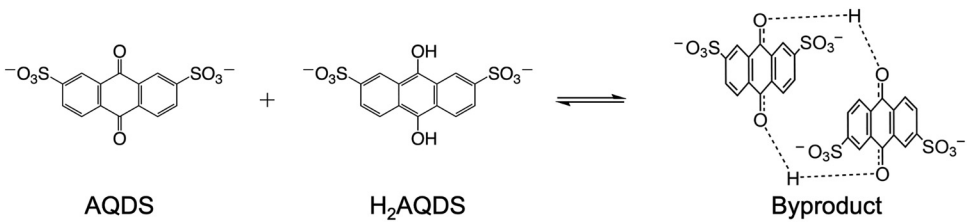

Fig. 16 Chemical structures of the AQDS/H_2AQ redox mediator and the quinone dimer byproduct formed at the anode. Reprinted with permission from ref. 27. Copyright (2025) American Chemical Society.

and cathode chambers to selectively transport Ca^{2+}.[21,29] However, Ca^{2+} transport into the high-pH catholyte interface precipitates operational failure. High interfacial pH (up to 12.4) induces heterogeneous $Ca(OH)_2$ nucleation directly on the membrane surface (Fig. 17a and b), physically blocking ion transport pathways (Fig. 17c).[24,26,29] This scaling drastically increases ohmic resistance, causing rapid voltage surges (>2 V within one hour) and system failure (Fig. 17d).[26] Additionally, strong interactions between divalent Ca^{2+} ions and fixed sulfonate groups cause membrane dehydration, embrittlement, and cracking,[26,44] reducing $Ca(OH)_2$ production efficiencies to as low as 59%.[29]

3.3. Advanced fouling mitigation strategies

Fouling mitigation strategies generally rely on material modification, electrolyte engineering, or mechanical intervention. Zhang *et al.*[26] addressed non-selective ion transport by developing a polyaniline (PANI)-modified Nafion 117 composite membrane. The protonated PANI layer creates a barrier to divalent Ca^{2+} transport *via* three synergistic mechanisms: electrostatic repulsion (Donnan exclusion), steric hindrance due to the larger hydrated radius of Ca^{2+} (0.412 nm) *versus* K^+ (0.331 nm), and the high energetic penalty for Ca^{2+} dehydration (ΔG_{dehy} = 1505 kJ mol^{-1}).[26,45,46] This "orthogonalized ion management" utilizes K^+ as the primary charge

Table 1 Comprehensive comparison of advanced electrochemical reactor designs for cement precursor synthesis

Performance metric	Two-chamber (pH modulated)	Three-compartment (OER)	Low-voltage (HOR)	Tandem system (orthogonalized ions)	Zero-gap (redox mediator)
Key innovation	Engineering the catholyte chemistry to induce bulk precipitation and prevent fouling.	Foundational three-chamber architecture establishing proof-of-concept.	H_2 recycling to a Hydrogen Oxidation Reaction (HOR) anode to reduce cell voltage.	Decouples precipitation into an external reactor *via* a Ca^{2+}-blocking composite membrane.	A (PCET) redox mediator in zero-gap architecture.
Reactor architecture	2-Compartments: a simple H-cell design with only anode and cathode chambers.	3-Compartments: Anode, cathode, and a central chemical chamber.	3-Compartments: Anode, cathode, and a central chemical chamber.	3-Compartment electrolyzer coupled to a separate external calcium reactor.	2-Compartments: a zero-gap design with only anode and cathode chambers.
Main membranes	A single standard CEM separates the two chambers.	BPM (separates anode/chemical) and a standard CEM (separates chemical/cathode).	Two CEMs (one replaces the BPM to conduct protons from the HOR anode).	BPM and a novel PANI-coated composite CEM that blocks Ca^{2+} transport.	A single PANI-coated CEM that blocks Ca^{2+} transport.
Electrode materials	Platinum plate electrodes for both anode and cathode.	Nickel foam for both anode and cathode.	Pt/C gas diffusion electrode (anode) and nickel foam (cathode).	Nickel foam for both anode and cathode.	Graphite felt for both anode and cathode.
Electrolyte system	Aqueous $NaNO_3$ with a Ca^{2+}-doped catholyte (0.2 M $Ca(NO_3)_2$).	Anode: 1.0 M KOH; center: $CaCO_3$ slurry in 1 M $CaCl_2$; cathode: 1.0 M KCl.	Anode: humidified H_2 gas; center: Ca CO_3 slurry in 1 M $CaCl_2$; cathode: 1.0 M KCl.	Anode: 1.0 M KOH; center: $CaCO_3$ slurry in 1 M KCl; cathode: 1.0 M KCl.	H_2O/MeCN with KOAc supporting salt.
Operating voltage (at 100 mA cm^{-2})	~3.5 V[a]	2.9 V	1.77 V	~5.0 V	0.38 V[b]
Current density	Up to 180 mA cm^{-2}	100 mA cm^{-2}	100 mA cm^{-2}	100 mA cm^{-2}	Tested up to 1 A cm^{-2}
Faradaic efficiency (%)	84%[c]	~100%	70–90%	100%	100%
Max production rate (of $Ca(OH)_2$)	1150 mg h^{-1}	486 mg h^{-1}	Not reported	Not reported[d]	Not reported[d]
Demonstrated stability	>12 hours	<1 hour	~5 hours	>50 hours	Not a focus of the study
Primary advantage	Highest reported production rate and a simple reactor design.	Generates pure, separate, and unmixed co-product streams.	Dramatically reduced cell voltage and overall energy consumption.	Long-term stability by eliminating *in situ* fouling.	Ultra-low cell voltage and extremely high energy efficiency.
Key limitation	Requires manual pH cycling *via* intermittent stirring; produces a mixed gas output.	Severe and rapid membrane fouling; high energy consumption due to OER/BPM overpotentials.	Lower Faradaic efficiency due to parasitic proton currents; requires expensive platinum catalyst.	Higher system complexity due to the external reactor and high cell voltage.	Requires organic redox mediators, solvents, and elevated temperatures.
Reference(s)	Xu *et al.*[29]	Zhang *et al.*[21]	Mowbray *et al.*[30]	Zhang *et al.*[26]	Ji *et al.*[27]

[a] The source paper also reports a 9 V test, which was an accelerated experiment to observe fouling dynamics. The ~3.5 V value is more representative of the standard H-cell operation for this chemistry. [b] The record-low 0.38 V was achieved under optimized conditions, including a mixed-solvent electrolyte and an elevated operating temperature of 60 °C. [c] This refers to the faradaic efficiency for $Ca(OH)_2$ production. The key achievement was improving this value from a baseline of 59% (in a fouled system) to 84% by successfully mitigating membrane fouling through electrolyte engineering. [d] For the Tandem and zero-gap systems, the final $Ca(OH)_2$ product is formed in a separate, external reactor. The studies focused on demonstrating the stability and energy efficiency of the electrolyzer itself, so an equivalent *in situ* production rate was not provided as a primary KPI.

carrier, effectively decoupling electrolysis from precipitation and enabling stable operation for over 50 hours (Fig. 18).

Alternatively, electrolyte engineering allows for fouling control without modification. Xu *et al.*[29] demonstrated that doping the catholyte with 0.2 M $Ca(NO_3)_2$ induces $Ca(OH)_2$ precipitation in the bulk solution rather than at the membrane interface. This approach buffers the local pH to ~11.8, preventing scaling and increasing Faradaic efficiency from 59% to 84%. Anodic fouling was concurrently managed *via* intermittent stirring to induce pH-driven dissolution.

A third, more direct approach focuses on physically preventing precipitate accumulation through mechanical and hydrodynamic forces. Miao *et al.*[32] integrated a continuous NaCl electrolyte flush with an *in operando* mechanical wiper to physically clear membrane surfaces (Fig. 19A and B). This configuration sustained stable operation at high current densities (200 mA cm^{-2}) for over 13 hours (Table 2).

4. Performance characteristics and scaling considerations

4.1. Energy efficiency and performance metrics

A reactor's performance is defined by its energy efficiency, governed by cell voltage (E_{cell}), and its performance metrics, namely current density (j) for rate and Faradaic efficiency (FE) for yield. The baseline for this technology is the three-compartment OER flow electrolyzer detailed by Zhang *et al.*[21]

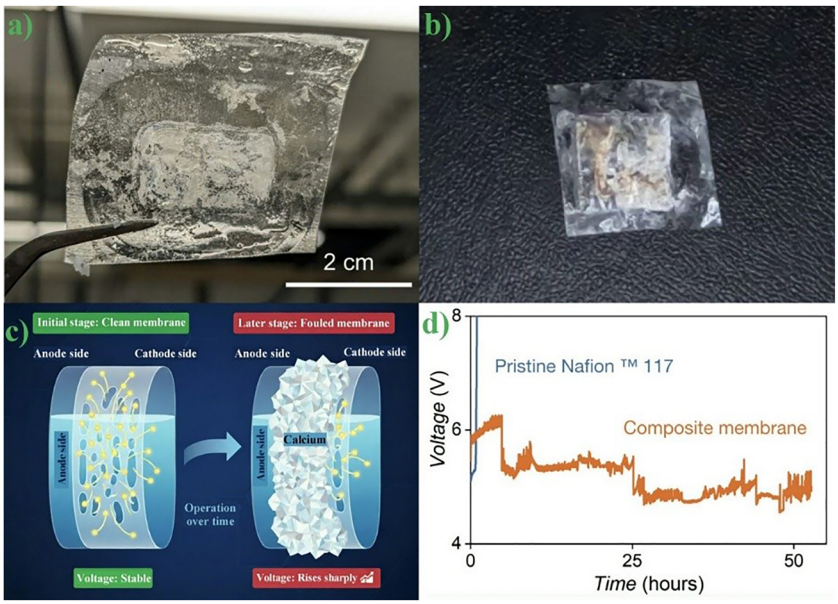

Fig. 17 Mechanism and impact of CEM fouling. (a) Optical micrograph of ($Ca(OH)_2$) deposition on a Nafion™ 117 membrane. Reprinted with permission from ref. 26. Copyright (2025) the Royal Society of Chemistry. (b) Calcium scaling on an Aquivion membrane after 44 hours.[1] (c) Schematic of physical ion transport blockage. (d) Rapid voltage increase caused by fouling-induced ohmic resistance. Reprinted with permission from ref. 26. Copyright (2025) the Royal Society of Chemistry.

Operating at 100 mA cm^{-2}, it achieved near-100% FE but required a high cell voltage of 2.9–4.2 V (Fig. 20). This resulted in substantial energy consumption (>800 kWh ton^{-1}) due to large overpotentials from the oxygen evolution reaction (OER) and the bipolar membrane (BPM).[30] A pivotal advancement was the development of a low-voltage three-compartment system that replaces the OER anode with the HOR anode, recycling cathodic H_2 to generate protons.[30] This modification radically reduced the cell voltage to 1.77 V at 100 mA cm^{-2}. As shown in Fig. 21, this improvement is directly attributable to the minimal 0.11 V overpotential of the HOR anode and its adjacent CEM, in stark contrast to the 1.14 V from the OER/BPM combination, lowering projected energy consumption to $\sim$600 kWh t^{-1}. However, this gain in voltage efficiency was offset by a reduced FE of 70–90%, attributed to parasitic proton crossover.

4.2. Product quality and utilization

Extensive characterization has confirmed the high quality of both the solid $Ca(OH)_2$ precursor and the gaseous co-products. The electrochemically produced solid has been identified as high-purity, crystalline $Ca(OH)_2$ (portlandite), with only trace amounts of $CaCO_3$ or residual electrolyte salts.[21,24,29,32] The product precipitates as fine particles, often with hexagonal crystal morphologies, in a size range suitable for downstream thermal processing.[24,28,29] Ellis *et al.*[24] confirmed that this $Ca(OH)_2$ readily decomposes to CaO and reacts with silica to form alite ($3CaO{\cdot}SiO_2$), validating its chemical compatibility. Ramirez-Amaya *et al.*[31] highlighted the process's ability to function as a purification mechanism. When processing low-quality industrial limestones with $CaCO_3$ content as low as 68%, the resulting solid $Ca(OH)_2$ precipitate was consistently purer, with diminished levels of contaminants like silica and alumina. This demonstrates that the process selectively isolates the calcium component, operating as a combined "CaO concentrator" and "pre-calciner". A key advantage of the three-compartment reactor design is its ability to generate three separate, high-purity gas streams: O_2 from the anolyte, H_2 from the catholyte, and CO_2 from the chemical chamber. Zhang *et al.*[21] fed the pure CO_2 stream directly into a second CO_2 reduction (CO_2RR) electrolyzer, converting over 60% to CO without intermediate purification.

4.3. Long-term stability and durability

The research frontier has shifted toward ensuring long-term durability. The primary concern is the chemical stability of the membranes. Long-term exposure to the highly alkaline catholyte can cause degradation of the polymer backbone in anion exchange membranes.[28] Similarly, prolonged exposure and ion exchange with Ca^{2+} can lead to gradual embrittlement and dehydration of CEMs.[26,44] Electrode durability is also a key consideration. While specialized dimensionally stable anodes (like IrO_2) and catalyzed cathodes (Pt/C) have shown structural integrity after extended testing,[32] the long-term abrasion resistance of cost-effective materials like nickel foam in continuous slurry-fed systems needs to be validated. Ensuring the longevity of system components under conditions of continuous thermal and chemical stress will be essential.

5. Life cycle assessment and techno-economic viability

The commercial deployment of electrochemical cement is contingent upon its economic competitiveness with the incumbent

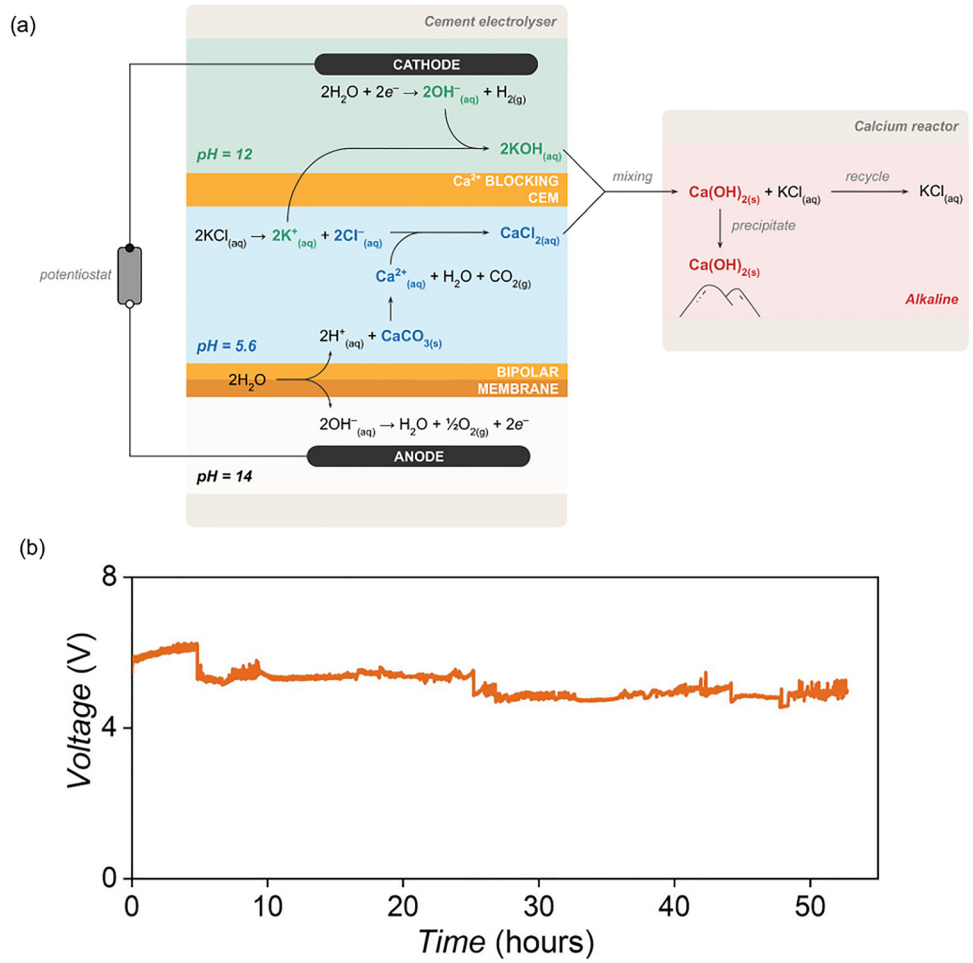

Fig. 18 Fouling mitigation *via* orthogonalized ion vectors. (a) Schematic of the composite PANI-CEM selectively blocking Ca^{2+} to decouple precipitation from electrolysis. (b) Voltage stability over 50 hours at 100 mA cm^{-2}, demonstrating the elimination of fouling-induced degradation. Reprinted with permission from ref. 26. Copyright (2025) the Royal Society of Chemistry.

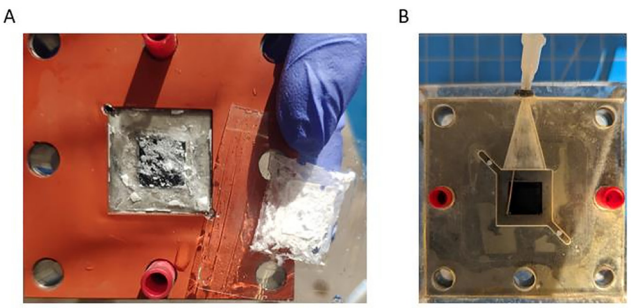

Fig. 19 This figure demonstrates a mechanical strategy to counteract the accumulation of $Ca(OH)_2$ precipitate (A) observed during stability tests. The solution is a custom flow field with an integrated wiper (B) designed for *in operando* cleaning of the electrolyzer. Reprinted with permission from ref. 32. Copyright (2023) American Chemical Society.

thermal process. Techno-economic analyses (TEAs) indicate that while current costs exceed those of conventional production, pathways to economic parity are achievable through improved reactor energy efficiency, low-cost renewable electricity, and carbon pricing. Consequently, economic viability relies on the convergence of technology maturation and supportive market mechanisms rather than fundamental process limitations.

5.1. Carbon footprint analysis and life cycle assessment (LCA)

The primary motivation for developing electrochemical cement technologies is their profound environmental benefit. The conventional thermal process has a carbon footprint of approximately 800–900 kg of CO_2 per ton of cement, with process emissions from limestone calcination accounting for ~60% and fuel combustion for ~30%.[20,21,32] Electrochemical routes fundamentally alter this paradigm by capturing process CO_2 and replacing fossil fuel combustion with clean electricity. A comparative LCA, summarized in Fig. 22, quantifies this advantage across different electrochemical pathways and electricity grid scenarios. Key findings include:

- Electrochemical routes powered by the current global average grid still offer significant emissions reductions compared to the conventional thermal process.
- When coupled with low-carbon grids (*e.g.*, Canada's grid), the projected footprint of the anion-mediated ECE process drops to approximately 200 kg CO_2 per ton.

Table 2 Comprehensive comparison of advanced membrane fouling mitigation strategies

Strategy name	Key innovation	Underlying mechanism	Key performance result	Ref.
Orthogonalized ion vectors (tandem reactor)	PANI-coated composite CEM that blocks Ca^{2+} transport.	Spatially decouples precipitation from electrolysis. K^+ ions serve as the primary charge carrier in the CEM. Ca^{2+} across and OH^- are mixed in an external reactor.	Sustained, stable operation for 50^+ hours at 100 mA cm^{-2} with no voltage increase. Eliminated the primary cause of operational instability.	Zhang *et al.*[26]
Electrolyte engineering & pH modulation	Controlled addition of Ca^{2+} ions (0.2 M) directly into the catholyte.	Promotes bulk precipitation of $Ca(OH)_2$ away from the membrane interface, buffering the local pH from 12.4 down to 11.8.	Completely eliminated cathode-side membrane fouling. Boosted Faradaic efficiency for $Ca(OH)_2$ production from 59% to 84%.	Xu *et al.*[29]
Mechanical & hydrodynamic control	Combination of a continuous electrolyte flush and an *in operando* mechanical wiper.	Physically prevents precipitate accumulation on surfaces and actively removes any solids that do form without halting operation.	Enabled stable continuous operation for over 13 hours at a high current density of 200 mA cm^{-2}.	Miao *et al.*[32]

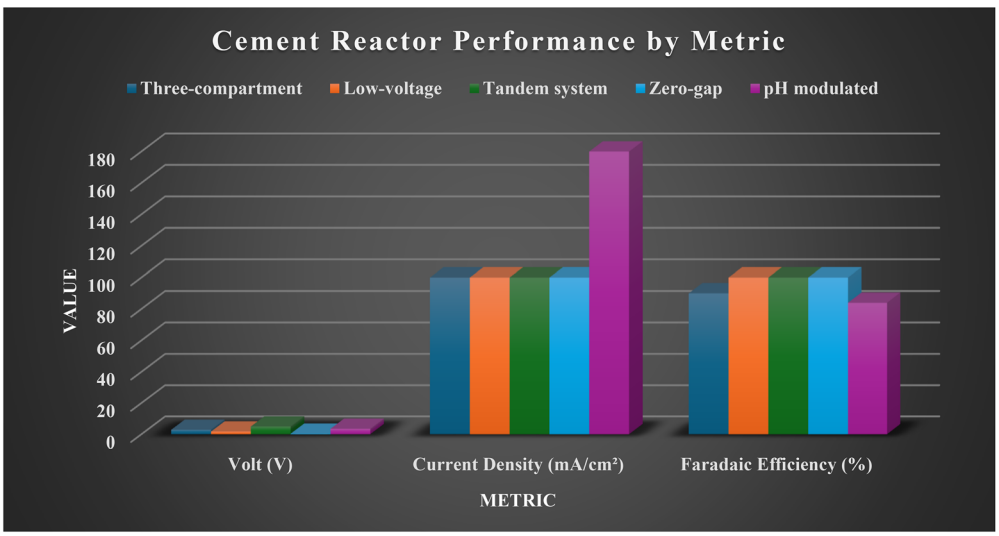

Fig. 20 Performance comparison of different electrochemical cement reactor designs across three key metrics: cell voltage, current density, and Faradaic efficiency (FE).

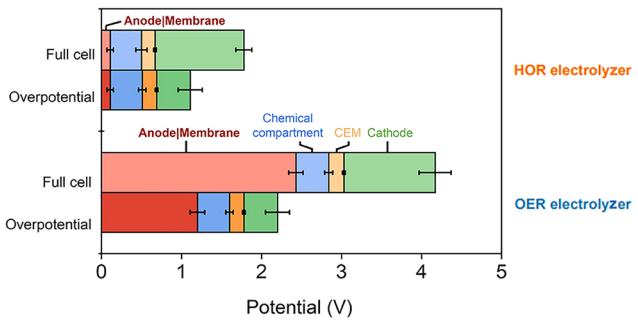

Fig. 21 Breakdown of voltage contributions for HOR and OER electrolyzers operating at 100 mA cm^{-2}. The bars are color-coded to identify specific component losses: red for the anode and adjacent membrane, blue for the central chemical compartment, orange for the CEM, and green for the cathode. The comparison reveals that the HOR system's superior efficiency is driven by the red segment, where the combined anode/membrane overpotential is reduced to just 0.11 V, in stark contrast to the 1.14 V required by the OER configurationReprinted with permission fromf. Reprinted with permission from ref. 30. Copyright (2023) American Chemical Society.

• In an optimistic scenario powered exclusively by solar electricity, the carbon footprint plummets to 149 kg CO_2 per ton for the OER pathway and to well below 100 kg CO_2 per ton for the ECE process.[30,32]

This represents a potential emissions reduction of over 90% compared to the incumbent method, demonstrating the profound potential for deep industrial decarbonization when these technologies are synergistically integrated with renewable energy infrastructure.

5.2. Cost structure and pathways to cost-parity

5.2.1. CAPEX and OPEX breakdown. The cost of producing electrochemical cement is composed of the initial capital expenditure (CAPEX) for the plant and the ongoing operational expenditure (OPEX) for materials and energy. Detailed models, primarily from Mowbray *et al.*[30] and Miao *et al.*,[32] provide a clear breakdown of these components for a reference plant with a production capacity of 3000 to 4100 tons of cement per day.

Capital expenditure for the electrolyzer plant is the largest initial investment. Based on the Department of Energy H2A cost model for water electrolyzers, a 3000 ton per day plant is

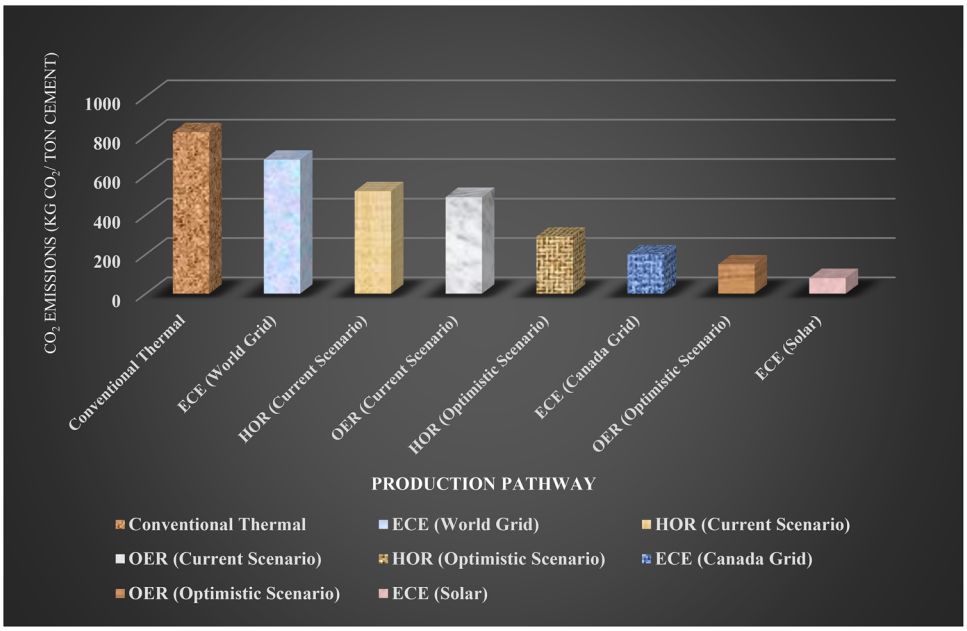

Fig. 22 Life cycle CO_2 emissions per ton of cement for the conventional thermal process benchmarked against various electrochemical pathways (OER, HOR, and ECE). The electrochemical routes are evaluated under different electricity grid scenarios: the global average, a low-carbon grid (Canada), and a fully renewable solar-powered grid. The analysis highlights that coupling electrochemical production with solar energy can reduce the carbon footprint from over 800 kg CO_2 per ton to well below 100 kg CO_2 per ton, representing a potential emissions reduction of over 90%.[30,32]

estimated to have a total installed CAPEX of 326 million dollars for an OER system and 335 million dollars for an HOR system.[30] This comprehensive figure includes the electrolyzer unit itself, which is estimated to cost between $16M for the OER system and twenty million dollars for the HOR system, a carbon dioxide compression unit at approximately 9.2 million dollars, the balance of plant (including piping and control systems) at around $10M, and significant contingency, indirect, and ownership costs which account for 40% of the total.[30] The higher capital expenditure for the HOR system is directly attributed to the more expensive platinum-group metal catalysts required for the hydrogen oxidation reaction at the anode.[30] A separate techno-economic analysis for the anion-mediated ECE process projects a capital cost of approximately $50 per ton (Fig. 23) representing a significant component of its total production cost.[32] However, it is a critical limitation of this specific model that it excludes the operational costs associated with treating and regenerating the acidic electrolyte, which would need to be accounted for in a complete system-level assessment.

Operational expenditure is overwhelmingly dominated by the cost of electricity. Across all electrochemical pathways, electricity is the largest and most sensitive cost component. For instance, in the techno-economic analysis for the anion-mediated ECE process, electricity is the largest single cost bar, exceeding capital cost, catalyst replacement, and chemical inputs combined.[32] Other operational costs include mineral feedstocks, such as limestone at approximately $12 per ton and clay at sixteen dollars per ton, periodic catalyst and membrane replacement (membranes have an estimated five-year lifespan), water, labor, and maintenance.[30,32]

5.2.2. Comparative economics and scenarios for cost-parity. Techno-economic models reveal clear pathways to competitiveness with the conventional thermal process, which has a benchmark production cost of approximately 113 to 120 per ton, a relationship detailed in Fig. 25.[21,30] The choice of electrochemical pathway is critical; for instance, using the hydrogen byproduct to power a low-voltage HOR system is projected to yield a cost reduction of $36 per ton compared to using it as a simple kiln fuel in an OER system. This saving directly results from the HOR pathway's lower electricity demand of $\sim$600 kWh t^{-1}, compared to over 800 kWh t^{-1} for the OER design. Sensitivity analyses confirm that the price of electricity and carbon are the most influential variables on economic viability.[30]

Under a "*Current Market Scenario*" (defined by $0.05 per kWh electricity and a $50 per ton carbon tax), electrochemical routes remain more expensive. The HOR pathway is the most competitive with a production cost of approximately $189 per ton, compared to $225 per ton for the OER pathway (Fig. 24a). In this case, the significant electricity savings from the HOR's lower voltage outweigh the cost of using natural gas for the kiln.[30]

Conversely, under an "*Optimistic/Cost-Parity Scenario*" (defined by $0.02 per kWh electricity and an $85 per ton carbon tax), the economic landscape inverts. Production costs become highly competitive, with the OER pathway at approximately $122 per ton (Fig. 24b) becoming slightly cheaper than the HOR pathway at $123 per ton. With inexpensive electricity, the HOR pathway's energy savings are less impactful, and its reliance on natural gas (which now incurs a high carbon tax) becomes a liability.[30]

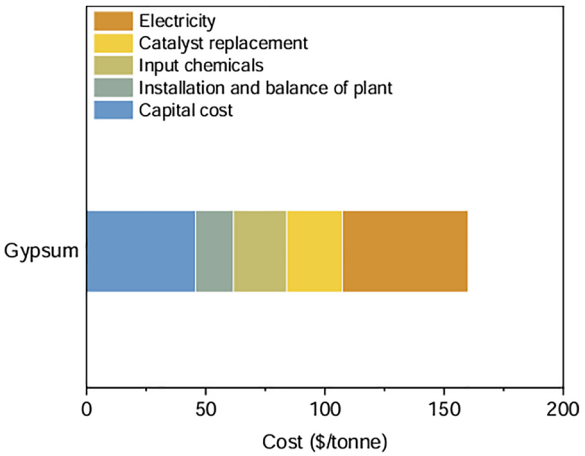

Fig. 23 A techno-economic assessment was conducted for the ECE process where gypsum serves as the primary feedstock. It is important to note that this analysis excludes the costs for acidic electrolyte treatment. Reprinted with permission from ref. 32. Copyright (2023) American Chemical Society.

These models collectively demonstrate that a carbon tax of approximately $50 per ton, combined with a renewable electricity price of two cents per kilowatt-hour, is sufficient to achieve cost-parity with incumbent manufacturing. Crucially, these analyses do not include the cost of post-combustion carbon capture for conventional plants, which is estimated to add an additional $90 per ton, making electrochemical routes significantly more favorable in a carbon-constrained world.[21,24,32]

5.3. Technology learning curves and commercialization pathways

Long-term commercial success hinges on future cost reductions and a strategic approach to market entry. Current techno-economic analyses are based on mature electrolyzer technology, but significant cost reductions are projected. Following the precedent of renewable energy sectors like solar photovoltaics, electrolyzer costs are expected to decline substantially, by as much as 50–70% by 2030, due to manufacturing scale economies, design optimization, and technological advances. This "technology learning curve" will be a major driver in reducing the overall capital investment required, accelerating the pathway to widespread commercial deployment.[46,47] The technology can be deployed either as a retrofit to existing cement plants, replacing the carbon-intensive precalciner, or in new, fully optimized greenfield facilities. Initial market entry should target specialty applications and premium market segments where the low-carbon footprint is a primary value driver. The quantified environmental benefit provides a powerful incentive for adoption through government procurement programs for "green cement" and green building certifications, which can justify a "green premium" on the selling price.

6. System integration and optimization for electrified cement production

The commercial viability of a decarbonized cement industry requires a shift from optimizing individual reactors to developing integrated, system-level architectures. This approach depends on the synergistic integration of the process with renewable energy infrastructure, circular material flows, and advanced carbon management strategies.[2] Key integration pathways, including electrified calcium looping, scalable production models, and the strategic valorization of co-products like green hydrogen, are examined in this section.

6.1. System-level integration architectures

The design of a zero-emission cement plant will involve a hybrid of emerging technologies. A key challenge in conventional decarbonization is capturing CO_2 from flue gas, which is heavily diluted with nitrogen from the air. A common strategy to address this is oxyfuel combustion, where fuel is burned in nearly pure oxygen. This eliminates nitrogen, producing CO_2-rich flue gas that is easy to process but requires an energy-

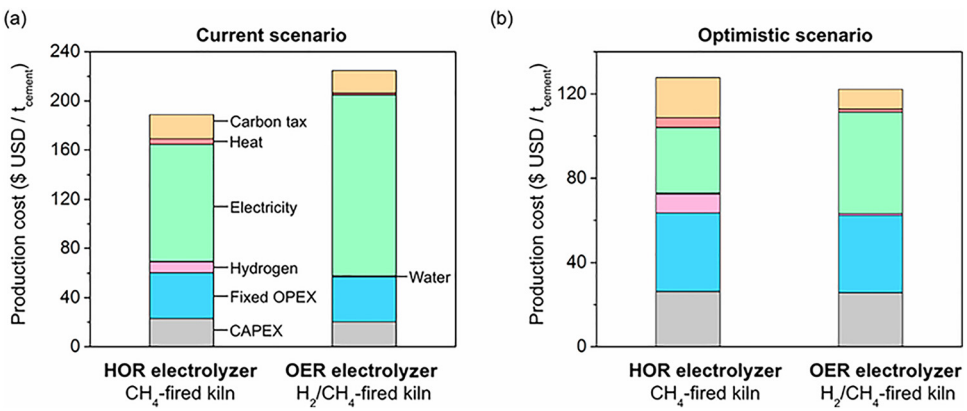

Fig. 24 Techno-economic comparison of electrochemical cement production using HOR and OER electrolyzers. The costs, broken down by CAPEX and OPEX components, are evaluated under two distinct scenarios: (a) a Current Market Scenario reflecting existing energy/carbon economics and (b) an Optimistic Future Projection based on low-cost solar power and stringent climate policy. Reprinted with permission from ref. 30. Copyright (2023) American Chemical Society.

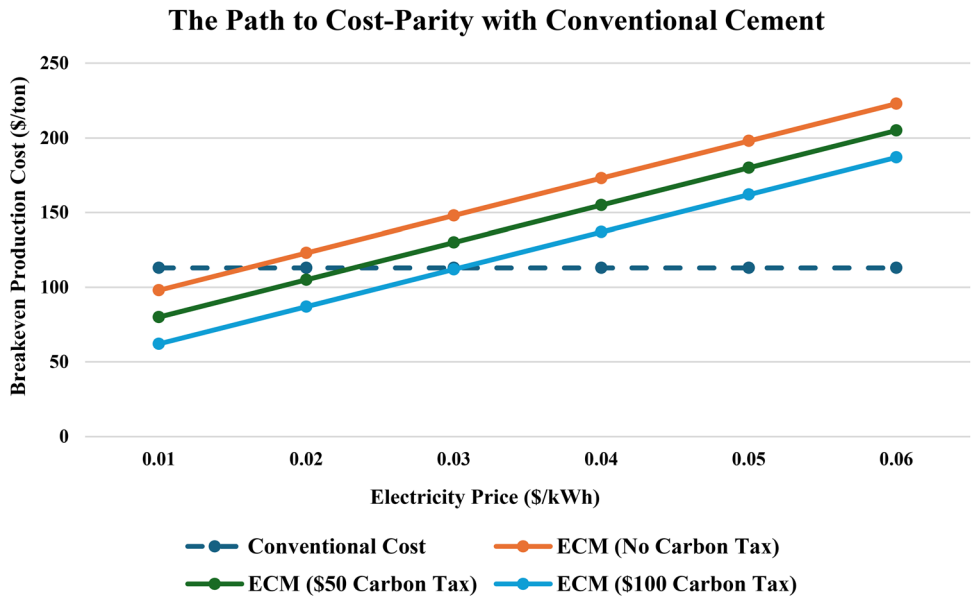

Fig. 25 Breakeven production cost for the electrochemical HOR pathway as a function of electricity price, evaluated under three carbon tax scenarios ($0, $50, and 100 per ton of CO_2). The horizontal dashed line represents the benchmark cost of conventional cement.[21,30]

intensive and costly Air Separation Unit (ASU) to supply the oxygen.

A more promising pathway that avoids this issue is the electrification of the calciner, specifically through an architecture known as electrified Calcium Looping with Thermal Energy Storage (CaL-TES), illustrated in Fig. 26.[2,13,48,49] Instead of burning fuel, this system uses low-cost renewable electricity to heat a storage medium (*e.g.*, $BaCO_3$/BaO) during off-peak hours. This stored thermal energy is then discharged on demand to provide the high-temperature heat required for the endothermic decomposition of $CaCO_3$. The primary advantage of this architecture is the elimination of the energy-intensive and costly Air Separation Unit (ASU) required for oxy-combustion, along with the complete abatement of fossil fuel-related emissions from the calcination process. Process modeling demonstrates that this electrified approach can significantly reduce the primary energy consumption. For an integrated configuration with 90% CO_2 capture efficiency, the primary energy demand decreases from 5320.9 MJ t^{-1}-clinker for an oxyfuel-based system to 4996.6 MJ t^{-1}-clinker for the electrified CaL-TES system. For a tail-end retrofit, the reduction is from 7458.0 MJ t^{-1}-clinker to 6484.0 MJ t^{-1}-clinker.[13,48,50] The system inherently produces a high-purity CO_2 stream directly from the calciner, making it ideal for subsequent utilization or sequestration without complex purification. The critical innovation is the TES unit, which decouples the continuous operational demand of the cement plant from the intermittent nature of renewable energy sources, thereby enhancing grid stability and economic feasibility.[13,48,50]

An alternative and potentially more transformative approach involves redesigning the process chemistry to utilize alternative, carbon-free feedstocks, enabled by direct electrification (Fig. 27).[1] The work by Lu *et al.*[1] demonstrates a scalable electrochemical process that uses carbon-free calcium silicates, sourced from abundant minerals or recycled concrete, as the primary feedstock instead of limestone. Water electrolysis, powered by renewable electricity, generates the pH gradient necessary to leach Ca^{2+} ions from the silicates and facilitate the mineralization of atmospheric or captured CO_2 into carbon-negative $CaCO_3$. This electrified materials production scheme offers several advantages:

1. Circular economy: it directly integrates recycled concrete fines, transforming a major construction waste stream into a valuable feedstock, thus reducing landfilling and the need for virgin material extraction.[1] This aligns with the principles of a circular economy, as highlighted by broader sustainability assessments.[51]

2. Co-product valorization: the process co-produces high-purity amorphous silica, a valuable supplementary cementitious material (SCM), and green hydrogen. This hydrogen can be used as a clean fuel for the final kiln step or as a chemical agent, creating multiple revenue streams from a single process.[1,52]

3. Process intensification: by utilizing technologies such as zero-gap electrolyzers, the system can achieve higher current densities and improved energy efficiency, paving the way for more compact and scalable reactor designs compared to traditional flow cells.[1]

This approach represents a fundamental reinvention of the cement front-end, whereas the CaL-TES system is a more direct evolution of existing calcination technology. A comparative analysis reveals different trade-offs in technology readiness level (TRL), capital cost, and feedstock flexibility,[2] as summarized in Table 3. Three primary strategies are analyzed and compared: traditional industrial pathways augmented with post-combustion capture, a system based on CaL-TES, and

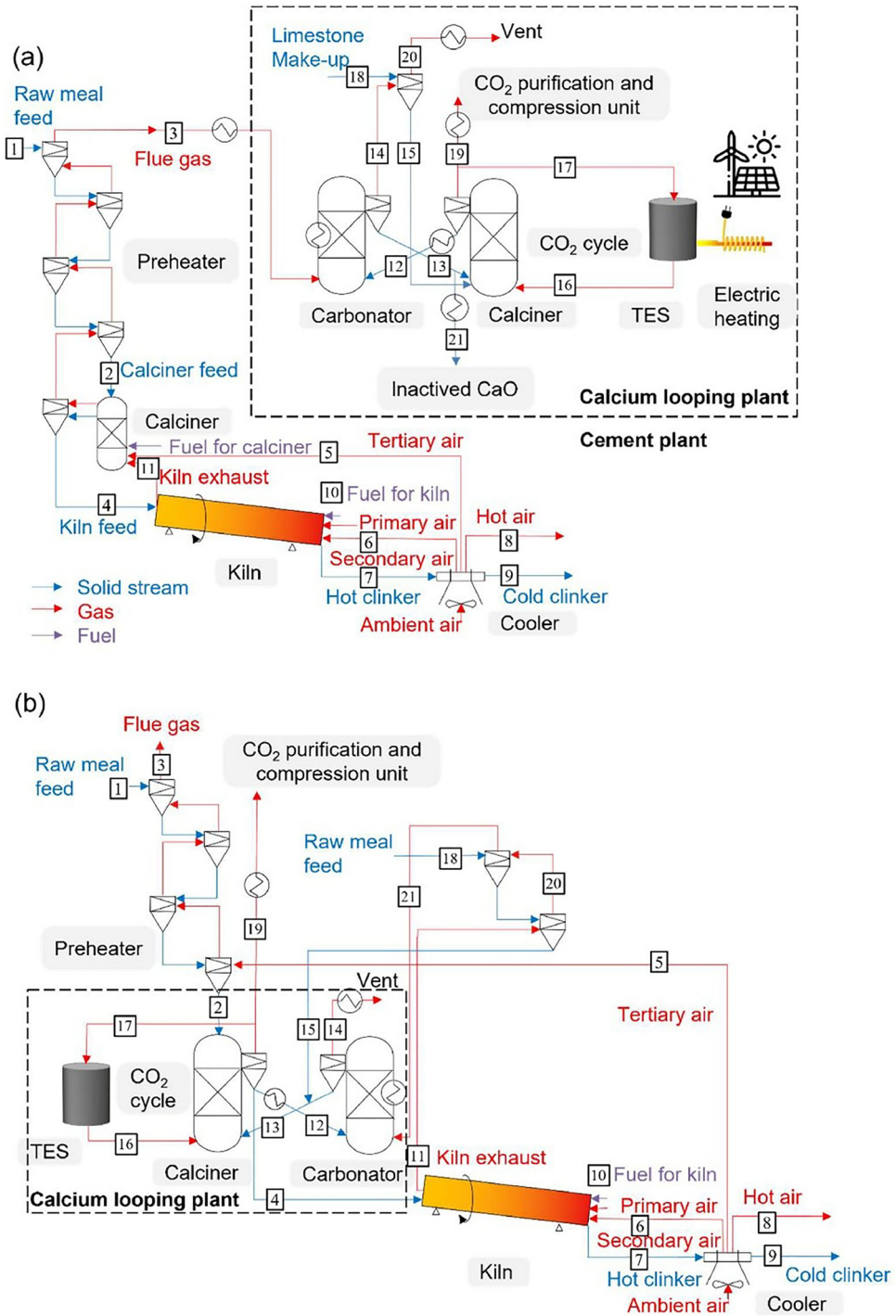

Fig. 26 Two configurations for deploying calcium looping in cement plants are (a) the tail-end setup, where the system treats flue gases after clinker production, and (b) the integrated setup, where it becomes a core part of the clinkering cycle itself. Reprinted with permission from ref. 48. Copyright (2023) Elsevier.

the direct electrification of materials obtained from alternative feedstocks.[1,2,48,51]

6.2. Co-product valorization and hydrogen integration

A fully optimized business model must also include the valorization of all high-purity co-products. As detailed in Table 4, the creation of additional revenue streams from the sale of hydrogen, oxygen, and valorized carbon dioxide will drastically improve overall project economics and accelerate the technology's path to widespread adoption.[53–55] Green hydrogen, co-produced from electrified processes,[1] is not merely a byproduct but a key enabler for deep decarbonization across hard-to-abate

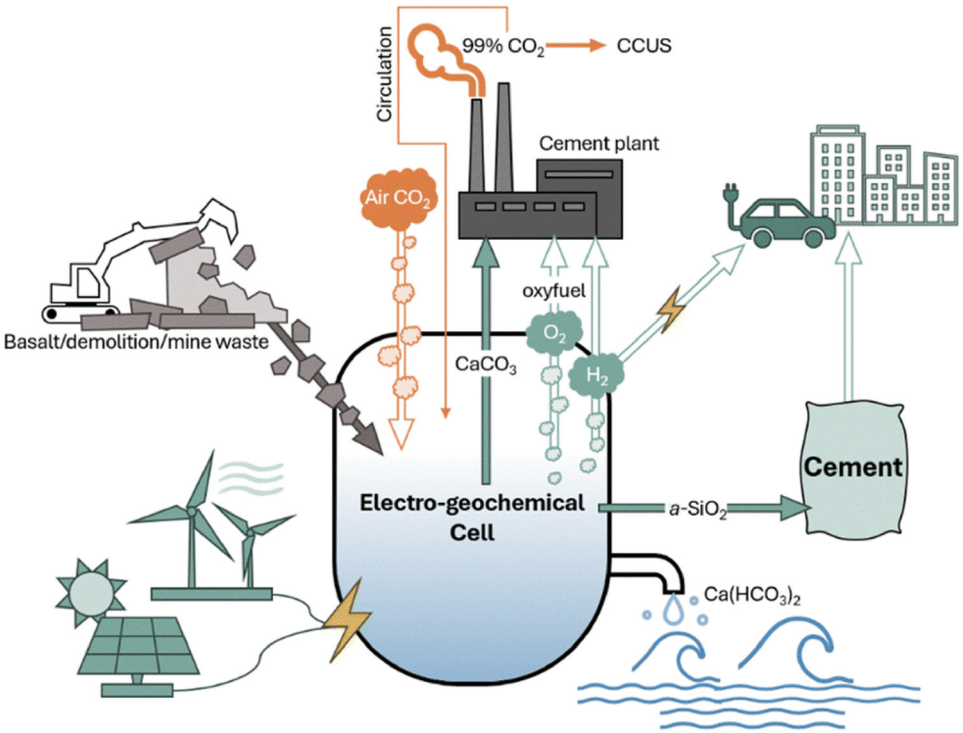

Fig. 27 A system-level diagram illustrating the direct electrification pathway for cement production. The process uses renewable electricity to power an electro-geochemical cell that converts Ca-bearing silicates (from industrial waste, rocks, or recycled concrete) into carbon-negative $CaCO_3$, amorphous silica (a-SiO_2), and green hydrogen (H_2), creating a circular material and energy flow.[1]

Table 3 Comparative framework of key electrification pathways for cement decarbonization

Feature	Electrified CaL-TES	Direct material electrification	Conventional (with post-combustion capture)
Primary feedstock	Limestone ($CaCO_3$)	Calcium silicates (*e.g.*, wollastonite, recycled concrete)	Limestone ($CaCO_3$)
Electrification point	Calciner heating (indirect)	Water electrolysis & material leaching (Direct)	Grid power for plant operations & capture unit
CO_2 abatement	Eliminates fuel use in calciner; produces a pure CO_2 stream	Eliminates limestone process emissions; mineralizes captured CO_2	Post-combustion scrubbing of flue gas
TRL (estimated)	4–6 (pilot/demonstration)	3–5 (lab/pilot)	7–9 (Commercial)
Key co-products	None (pure CO_2 is the primary output)	Green H_2, amorphous silica (SCM), carbon-negative $CaCO_3$	None
Key economic barrier	CAPEX of TES and electric heaters; cost of electricity	Scalability of electrolyzers; feedstock processing	High OPEX of capture solvent/process; energy penalty

sectors.[52] The complete green hydrogen supply chain, from generation to industrial application, is depicted in Fig. 28. In an integrated cement facility, it can be valorized through several high-impact pathways:

1. Clean fuel for clinkering: hydrogen can be used as a primary fuel or co-fired with natural gas in burners for the final, high-temperature clinkering stage. As a co-fuel, blending up to 20% H_2 by volume with natural gas is feasible with existing burner technology, offering a significant and immediate reduction in combustion-related CO_2 emissions without major retrofits.[52]

2. chemical reductant: beyond its role as a fuel, hydrogen's primary industrial application is as a chemical agent. In the steel industry, for example, it is poised to replace carbon as the reductant in the direct reduced iron (DRI) process. A next-generation DRI plant producing one million tons of steel annually would require a photovoltaic capacity of approximately 3200 MW to supply the necessary green hydrogen.[52] This demonstrates the massive scale of renewable energy required but also the transformative potential of integrating hydrogen-based chemistry into industrial processes, a model applicable to future cement production.

3. Energy storage and grid balancing: produced during periods of excess renewable generation, hydrogen can be stored (*e.g.*, in compressed gas tanks) and used to generate power during peak demand or when renewables are unavailable,

Table 4 Co-products of electrochemical cement synthesis and their utilization pathways

Co-product	Source/reactor compartment	Potential utilization strategies and benefits
Hydrogen (H_2)	Cathode (HER)	1. Kiln fuel: can be combusted with O_2 to provide carbon-free, high-temperature heat for the final sintering step, eliminating the need for fossil fuels.[21,24] 2. Anode fuel (HOR): can be recycled to the anode in an HOR-based reactor to dramatically lower the cell voltage and energy consumption.[30]
Oxygen (O_2)	Anode (OER)	Oxy-fuel combustion: can be used with H_2 or other fuels in the kiln to improve combustion efficiency, increase kiln throughput, and produce a CO_2-rich flue gas that is easier to capture.[24]
Carbon dioxide (CO_2)	Central chamber (limestone dissolution)	1. Direct sequestration: the pure, concentrated stream can be compressed and sequestered at a much lower energy and cost penalty compared to capturing dilute CO_2 from flue gas.[24] 2. Chemical valorization (CCU): can be used as a pure feedstock for downstream electrochemical or thermochemical processes (*e.g.*, CO_2RR) to produce value-added fuels and chemicals, creating a circular carbon economy.[21,42]

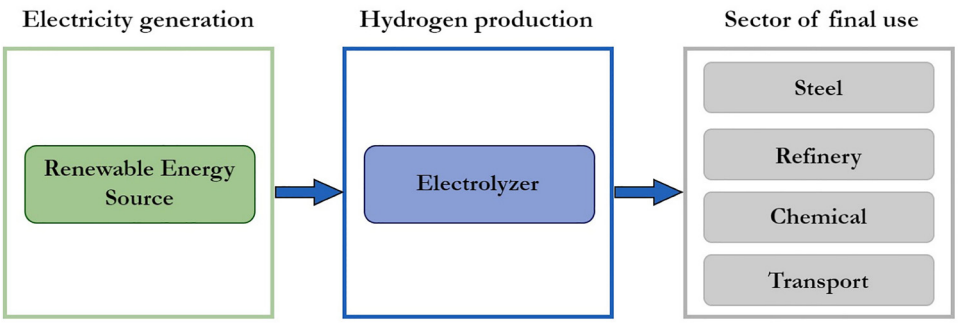

Fig. 28 An illustration that outlines the pathway of green hydrogen, beginning with renewable-powered electrolysis and ending with its final use. A key application is in the cement industry, where hydrogen acts as a valuable co-product for use as a clean fuel in clinkering or as a chemical agent in next-generation processes.[52]

serving a similar function to a TES but with greater flexibility for use as a fuel or chemical.[52,56]

6.3. Reactive carbon capture integration for CO_2 valorization

A key advantage of electrified calcination, such as the CaL-TES system, is the production of a high-purity (>95%) CO_2 stream, undiluted by nitrogen.[2,48] This captured CO_2, rather than being a liability requiring costly geological sequestration, can be treated as a valuable chemical feedstock, which is a concept central to carbon capture and utilization (CCU). Integrating reactive carbon capture pathways transforms the cement plant into a hub for producing carbon-based products, with the entire integrated system powered by low-carbon electricity.

Viable valorization pathways for this high-purity CO_2 stream include:

1. *Ex situ* mineral carbonation: the captured CO_2 is reacted with alkaline materials, such as industrial wastes (*e.g.*, steel slag) or the amorphous silica and calcium-rich byproducts from electrified material production pathways, to form stable carbonate minerals.[1] This process locks CO_2 into solid form, creating valuable construction materials like carbon-negative aggregates or next-generation SCMs, thereby establishing a circular carbon economy within the construction materials sector.[51]

2. Electrochemical conversion to fuels and chemicals (E-fuels): the pure CO_2 stream is an ideal feedstock for co-electrolysis with water or green hydrogen (potentially sourced from a co-located electrolyzer) to produce syngas (CO + H_2), methanol, or other platform chemicals.[1] The critical synergy lies in using the same low-cost, off-peak renewable electricity to power both the initial cement decarbonization and the subsequent energy-intensive CO_2 conversion, maximizing asset utilization and improving process economics.

3. Biological conversion: the CO_2 can serve as a nutrient for algae cultivation in photobioreactors to produce biofuels or high-value bioproducts. This pathway leverages photosynthesis to convert inorganic carbon into organic matter, integrating industrial processes with biological systems.

Reactive carbon capture (RCC) addresses standard CCU limitations by directly valorizing liquid-phase absorbents (*e.g.*, aqueous bicarbonate), thereby circumventing energy-intensive thermal regeneration.[57–59] To minimize ohmic resistance, a two-chamber, zero-gap architecture utilizing a bipolar membrane (BPM) has become the standard configuration (Fig. 29 and 30).[60–64] In this assembly, the BPM provides a proton flux to neutralize bicarbonate *in situ*, generating CO_2 (i-CO_2) for immediate reduction.[59,61,65–68] Unlike gas-fed systems, this design employs a hydrophilic porous cathode to facilitate liquid transport.[37,40,69] This approach offers significant advantages, including resilience to impurities such as SO_X and O_2 and single-pass CO_2 utilization efficiencies exceeding 40%.[70–73] However, widespread implementation is constrained by the thermodynamic pH mismatch between the capture and conversion steps and the voltage penalty associated with water dissociation at the BPM, which typically exceeds 3 V.[43,65]

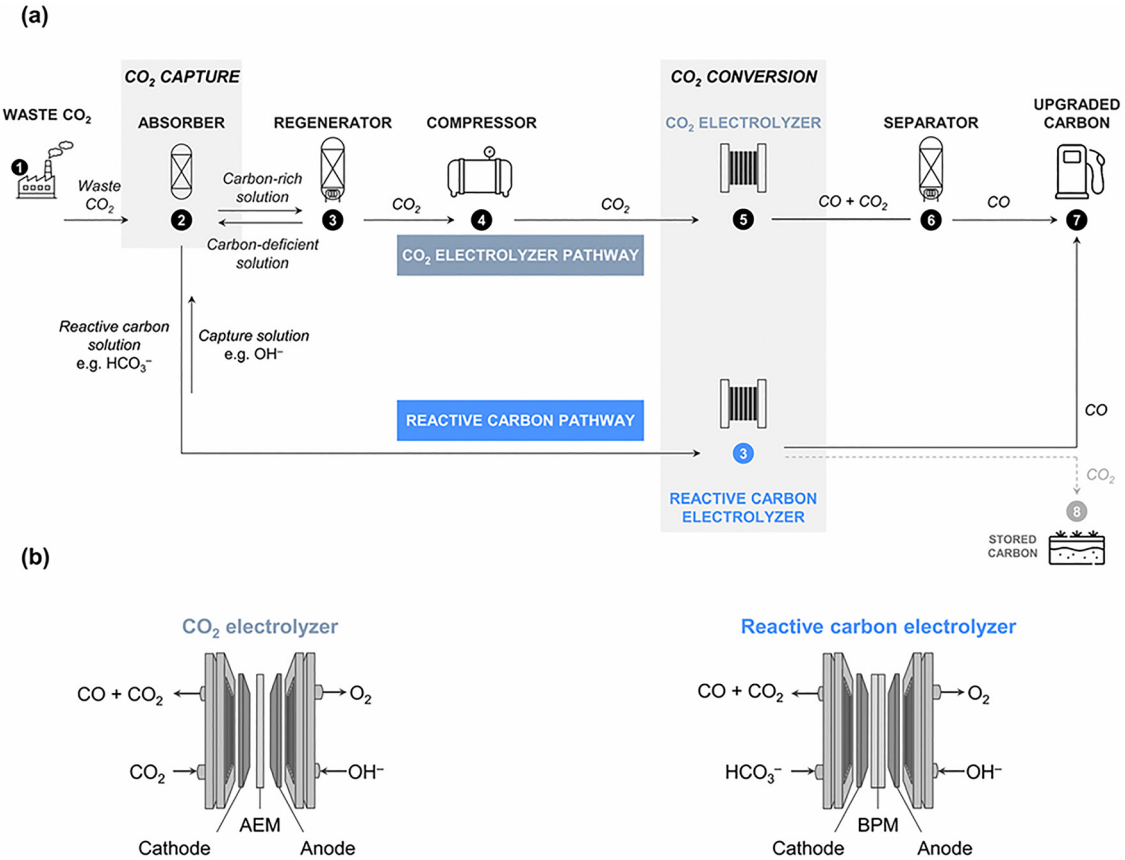

Fig. 29 (a) Comparison of CO_2 capture and utilization strategies. While both use alkaline absorption, the CO_2 electrolyzer requires thermal/vacuum regeneration to release gas, whereas the reactive carbon electrolyzer processes the liquid directly, avoiding gas liberation steps. (b) Cross-sectional view of electrolyzer components, including BPM and AEM. Reprinted with permission from ref. 59. Copyright (2024) the Royal Society of Chemistry.

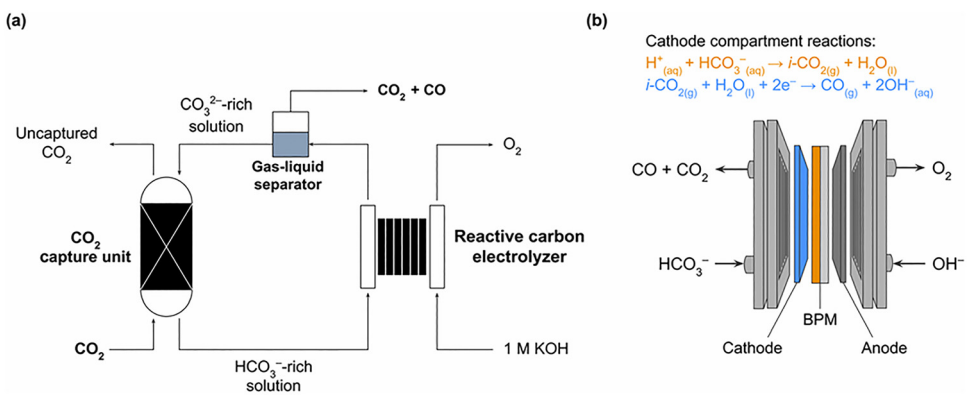

Fig. 30 (a) Integrated system for CO_2 capture and utilization: alkaline absorption of CO_2 produces a liquid eluent for direct transfer to the electrolyzer. (b) Reactive carbon electrolyzer cathode compartment shows i-CO_2 liberation *via* BPM and subsequent reduction to CO_2. Anode compartment fed with 1 M KOH. Reprinted with permission from ref. 59. Copyright (2024) the Royal Society of Chemistry.

A synergistic integration of these RCC systems with electrochemical cement production is proposed. Tandem cement electrolyzers inherently generate a Ca^{2+}-rich anolyte saturated with dissolved CO_2. This stream can serve directly as the liquid feedstock for a downstream RCC electrolyzer. Integrating these technologies establishes a closed-loop system where limestone-derived CO_2 is converted into fuels or chemicals (*e.g.*, syngas) rather than requiring sequestration. This coupling simultaneously recovers cement precursors and valorizes carbon, thereby enhancing the technoeconomic viability of zero-emission cement manufacturing.[26,33]

6.4. Renewable energy integration and grid dynamics

The deployment of electrified cement manufacturing is inextricably linked to the availability of massive-scale renewable energy.[2,56]

The intermittency of solar and wind power presents an operational challenge for cement plants, which traditionally operate continuously. The CaL-TES architecture provides a robust solution by using the TES unit as a thermal buffer. This enables the plant to draw power when it is cheapest and most abundant (*e.g.*, during peak solar insolation) and use that stored thermal energy to ensure the continuous operation of the calciner.[48]

This operational flexibility allows the cement plant to transform from a passive, baseload consumer into an active participant in the energy market. By scheduling charging cycles, the plant can provide valuable grid-balancing services, such as demand response (shifting consumption away from peak hours) and frequency regulation.[56] These ancillary services can create new revenue streams, offsetting the capital costs of the electrification and storage equipment.[48] This "virtual power plant" concept, integrating industrial loads with the grid (Fig. 31), is critical for stabilizing an electricity system with high penetration of renewables.[52]

6.5. Continuous assessment and process optimization

To manage the complexity of these integrated systems, a continuous assessment framework (as shown in Fig. 32) is essential. Inspired by IoT-enabled solutions (Fig. 33), this approach moves beyond static, one-time LCA/TEA studies to a dynamic, data-driven optimization model.[51] Sensors monitoring raw material inputs, energy consumption, and emissions feed real-time data into a cloud platform. Here, LCA and TEA templates are continuously updated, allowing process managers to:

- Optimize production schedules based on real-time electricity prices and renewable availability.
- Dynamically adjust feedstock blends (*e.g.*, Portland-limestone cement *vs.* OPC) to meet economic and environmental targets.
- Provide transparent, verifiable data for compliance reporting and sustainability certification.

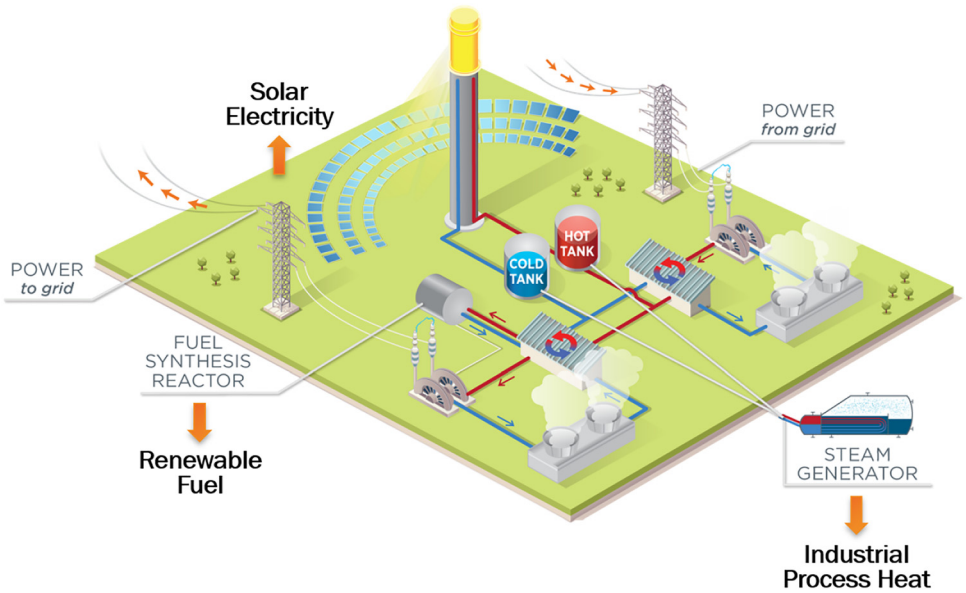

Fig. 31 U.S. Department of Energy schematic outlining diverse pathways for the integration of concentrated solar power into broad industrial applications.[2,74]

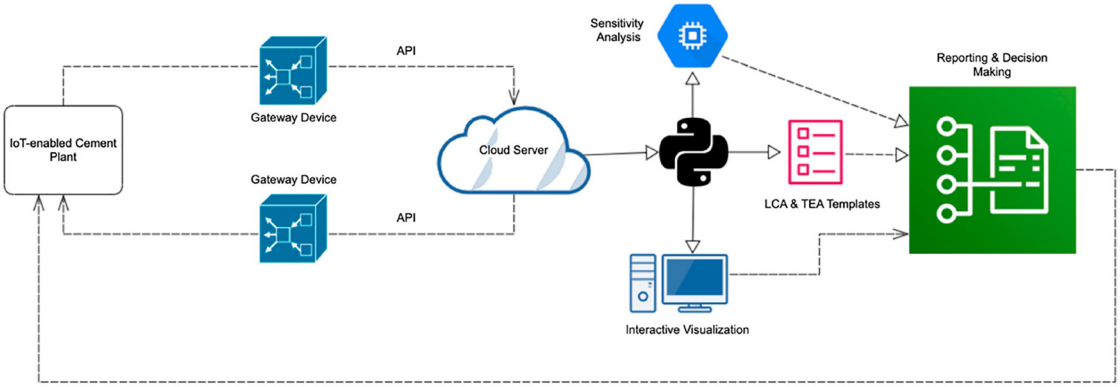

Fig. 32 A cyclical framework for ongoing assessment and enhancement.[51]

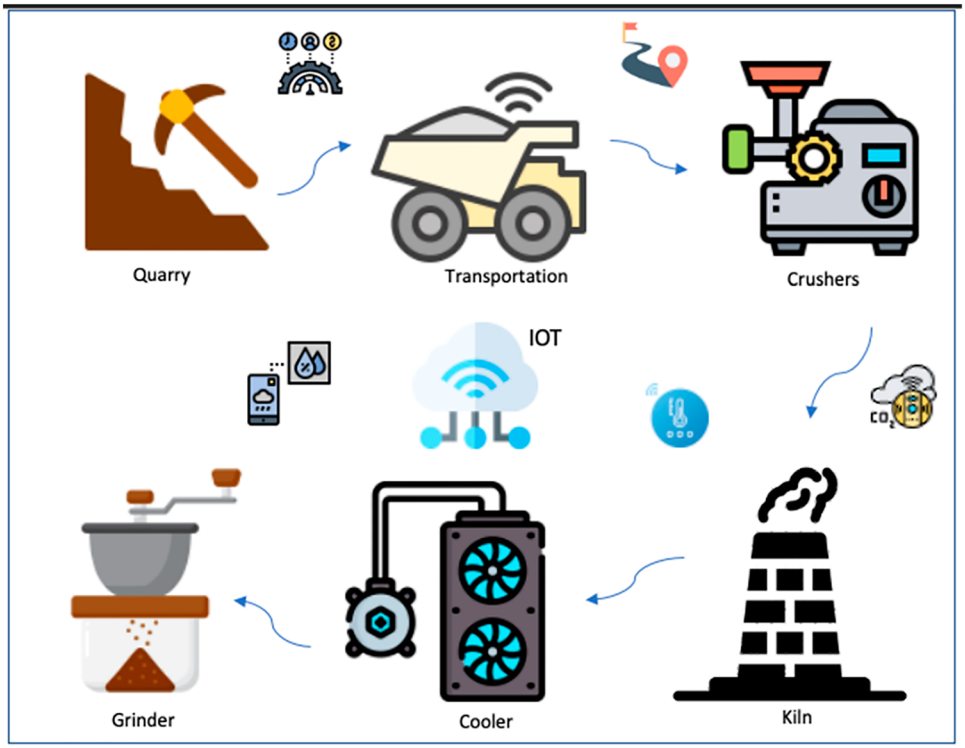

Fig. 33 IoT Integration in cement manufacturing.[51]

This data-driven feedback loop enables a cement plant to operate as a responsive, innovative, and sustainable business, capable of rapidly testing and validating new decarbonization strategies.[51]

7. Conclusions and strategic outlook

Electrochemical cement synthesis has matured into a viable decarbonization pathway. This section summarizes technological milestones, strategic priorities, and the transformative potential of the technology.

7.1. Technological maturity and performance benchmarks

Recent advancements have addressed critical voltage and stability challenges:

- Technological feasibility: laboratory systems have achieved 100% faradaic efficiency at 100 mA cm^{-2} with $Ca(OH)_2$ production rates of 486 mg h^{-1}.
- Energy efficiency: reactor innovation has reduced cell voltages from 2.9 V (OER) to 0.38 V (zero-gap), significantly lowering energy consumption.
- Operational stability: tandem configurations have effectively mitigated acute membrane fouling, demonstrating sustained operation for over 50 hours.

The diversity of successful reactor architectures, from three-compartment systems offering pure gas streams to tandem systems eliminating fouling and zero-gap designs minimizing energy consumption, provides multiple viable pathways for optimization and application-specific adaptation.

7.2. Critical challenges and strategic research priorities

Transitioning from laboratory demonstration to commercial deployment requires addressing specific technical and economic barriers.

7.2.1. Technical and materials science priorities. 1. Advanced membrane development: multi-year industrial lifetimes require fouling-resistant, low-cost materials. While perfluorinated sulfonic acid membranes (*e.g.*, Nafion) currently serve as the benchmark for laboratory-scale performance due to their chemical stability, their commercial deployment in the cement industry is likely prohibitive. The high cost of fluorinated polymers ($>\$500$ m^{-2}) aligns poorly with the economic constraints of a commodity market priced at $\sim\$120$ per ton. Furthermore, the intrinsic affinity of the sulfonate groups in Nafion for calcium ions exacerbates internal scaling and dehydration issues. Consequently, industrial viability is predicated not on Nafion, but on the transition toward low-cost, non-fluorinated hydrocarbon alternatives or robust composite membranes explicitly engineered for calcium tolerance.

2. Reactor design and scale-up: scaling from 10–100 cm^2 cells to >1 m^2 stacks requires resolving mass transport, thermal management, and current distribution nonuniformities *via* computational modeling and pilot validation.

3. Electrode durability and cost: the long-term stability and abrasion resistance of cost-effective, earth-abundant materials (*e.g.*, nickel in slurry-fed systems) must be validated to reduce reliance on precious metal catalysts.

7.2.2. Economic and market barriers. 1. High capital costs: with current estimates 2–3 times higher than conventional plants, high CAPEX remains the primary economic barrier.

Substantial cost reductions through technology maturation and manufacturing scale economies (''learning curve effects'') are essential.

2. Comprehensive cost modeling: future techno-economic analyses must account for ancillary operational expenditures, such as acidic electrolyte treatment, to ensure accurate financial projections.

3. Market acceptance and regulatory frameworks: adoption requires performance validation to update building codes and the establishment of standardized carbon accounting frameworks.

7.3. Future perspectives and transformative impact

The successful deployment of electrochemical cement synthesis has the potential to fundamentally transform the cement industry and contribute to broader industrial decarbonization.

• Industrial transformation: the technology targets the elimination of 2.8 Gt of annual CO_2 emissions and establishes a precedent for electrifying other high-temperature industries like steel and glass.

• System-level integration and the circular economy: integration with renewable energy, hydrogen value chains, and urban mining of construction waste supports a circular economy.

• Emerging technologies: future advancements will likely come from the integration of emerging technologies. AI-driven process control could optimize efficiency in real-time. Nanomaterials offer performance improvements in electrode and membrane design, while smart materials with adaptive properties could respond to operational changes to prevent fouling and extend lifetimes.

The convergence of technological capability, economic opportunity, and environmental necessity creates unprecedented potential for electrochemical cement synthesis. Realizing this transformative technology's potential requires a sustained and collaborative commitment from research institutions, industry partners, and policymakers to address the remaining challenges and accelerate the transition from laboratory innovation to global deployment.

Conflicts of interest

There are no conflicts to declare.

Data availability

No primary research results, software or code have been included and no new data were generated or analysed as part of this review.

Acknowledgements

The authors acknowledge the financial support of this work by the American University in Cairo (Climate Change Grant: CCI-Cycle 4-SSE-PHYS-N.A-.03).

References

1 X. K. Lu, W. Zhang, B. N. Ruggiero, L. C. Seitz and J. Li, Scalable electrified cementitious materials production and recycling, *Energy Environ. Sci.*, 2024, **17**(24), 9566–9579.
2 S. S. Volaity, B. K. Aylas-Paredes, T. Han, J. Huang, S. Sridhar and G. Sant, *et al.*, Towards decarbonization of cement industry: a critical review of electrification technologies for sustainable cement production, *NPJ Mater. Sustain.*, 2025, **3**(1), 23.
3 V. Petrova, Innovations in cement production: The road to sustainability and a circular economy, *Eurasia Proc. Sci. Technology Eng. Math.*, 2024, **29**, 295–303.
4 V. Mittal and L. Dosan, System Dynamics Modeling of Cement Industry Decarbonization Pathways: An Analysis of Carbon Reduction Strategies, *Sustainability*, 2025, **17**(15), 7128.
5 K. M. Ripley, F. H. Saadi and Z. L. H. Burke, Cost-motivated pathways towards near-term decarbonization of the cement industry, *RSC Sustainability*, 2025, **3**(1), 255–263.
6 M. Pisciotta, H. Pilorgé, J. Davids and P. Psarras, Opportunities for cement decarbonization, *Cleaner Eng. Technol.*, 2023, **15**, 100667.
7 F. A. Rodrigues and I. Joekes, Cement industry: sustainability, challenges and perspectives, *Environ. Chem. Lett.*, 2011, **9**(2), 151–166.
8 M. P. Pfleger, E. Radl and M. Vill, Untersuchungen zum CO_2-Speicherpotenzial von rezyklierten Gesteinskörnungen und Zementproben unter Zwangskarbonatisierung, *Beton-Stahlbetonbau*, 2023, **118**(8), 565–574.
9 R. M. Andrew, Global CO_2 emissions from cement production, 1928–2018, *Earth Syst. Sci. Data*, 2019, **11**(4), 1675–1710.
10 H. G. Van Oss and A. C. Padovani, Cement manufacture and the environment: part I: chemistry and technology, *J. Ind. Ecol.*, 2002, **6**(1), 89–105.
11 M. Zajac, J. Skocek, M. Ben Haha and J. Deja, CO_2 mineralization methods in cement and concrete industry, *Energies*, 2022, **15**(10), 3597.
12 C. Edwards, Concrete's carbon quandary, *Eng. Technol.*, 2022, **17**(3), 22–26.
13 X. Liu, X. Li and R. Yang, High-temperature thermal storage-based cement manufacturing for decarbonization, *Carbon Neutrality*, 2022, **1**(1), 29.
14 E. Worrell, L. Price, N. Martin, C. Hendriks and L. O. Meida, Carbon dioxide emissions from the global cement industry, *Annu. Rev. Energy Environ.*, 2001, **26**(1), 303–329.
15 M. N. AndrÉ, L. N. Berge, B. M. Popol, M. M. LÉOn, B. M. Lincoln and M. S. Emmanuel, *et al.*, The Lukala Cement Plant's Life Cycle Analysis: Towards A More Sustainable Production, *Igmin Res.*, 2024, **2**(10), 835–845.
16 The ''Paris agreement'' on climate change: An opportunity for cement sector to further reduce its CO_2 emissions, *2017 IEEE-IAS/PCA Cement Industry Technical Conference*, ed. P. Fonta, 2017.
17 N. J. Cramer, Mitigating carbon dioxide emissions in the cement industry through carbon capture and storage, 2019.

18 C. S. I. Iea, Technology roadmap low-carbon transition in the cement industry, France/WBCSD, Geneva, Switzerland IEA, Paris, 2018.
19 D. Cheng, D. M. Reiner, F. Yang, C. Cui, J. Meng and Y. Shan, *et al.*, Projecting future carbon emissions from cement production in developing countries, *Nat. Commun.*, 2023, **14**(1), 8213.
20 A. Mokhtar and M. Nasooti, A decision support tool for cement industry to select energy efficiency measures, *Energy Strategy Rev.*, 2020, **28**, 100458.
21 Z. Zhang, B. A. W. Mowbray, C. T. E. Parkyn, C. Waizenegger, A. S. R. Williams and E. W. Lees, *et al.*, Cement clinker precursor production in an electrolyser, *Energy Environ. Sci.*, 2022, **15**(12), 5129–5136.
22 N. Bahnasawy, S. Al Anany and N. K. Allam, Electrochemical catalysis for the production of green cement: towards decarbonizing the cement industry, *Catal. Sci. Technol.*, 2024, **14**(15), 4087–4105.
23 R. Rouxhet, M. Loudeche, R. Santoro and J. Proost, Low-temperature water electrolysis under a sustained ph-gradient for electrochemically-induced decarbonation of limestone into hydrated lime, *J. Electrochem. Soc.*, 2024, **171**(9), 094504.
24 L. D. Ellis, A. F. Badel, M. L. Chiang, R. J. Y. Park and Y.-M. Chiang, Toward electrochemical synthesis of cement-An electrolyzer-based process for decarbonating $CaCO_3$ while producing useful gas streams, *Proc. Natl. Acad. Sci. U. S. A.*, 2020, **117**(23), 12584–12591.
25 *Development of a new type of electrochemical reactor for low temperature lime and cement production*, ed. M. Loudeche, R. Rouxhet and J. Proost, The Electrochemical Society, Inc, 2023.
26 Z. Zhang, A. S. R. Williams, S. Ren, B. A. W. Mowbray, C. T. E. Parkyn and Y. Kim, *et al.*, Electrolytic cement clinker precursor production sustained through orthogonalization of ion vectors, *Energy Environ. Sci.*, 2025, **18**(5), 2395–2404.
27 T. Ji, S. Ren, G. Jiang, Y. Yang, S. Ma and C. E. B. Waizenegger, *et al.*, Limestone conversion to cement clinker precursor in a zero-gap electrolyzer, *J. Am. Chem. Soc.*, 2025, **147**(31), 27314–27322.
28 S. Chaurasia, S. R. Aravamuthan, D. Luo, B. Akuzum, J. Wei and E. Agar, Leveraging Flow-Assisted Electrochemistry to Decarbonize Calcium Hydroxide Production in Cement Manufacturing, *J. Electrochem. Soc.*, 2025, **172**(7), 073506.
29 L. Xu, L. Liu, Z. Fang, M. Chen, G. Ou and M. Suzuki, *et al.*, Electrolyte pH modulation for efficient and durable electrochemical cement clinker precursor production, *Green Chem.*, 2025, **27**(14), 3706–3714.
30 B. A. W. Mowbray, Z. B. Zhang, C. T. E. Parkyn and C. P. Berlinguette, Electrochemical Cement Clinker Precursor Production at Low Voltages, *ACS Energy Lett.*, 2023, **8**(4), 1772–1778.
31 D. Ramirez-Amaya, P. Dreyse, N. P. Martínez, P. F. Troncoso, I. Navarrete and M. Noël, *et al.*, Comparison of the electrochemical decarbonation of different-grade limestones used in cement manufacturing, *Cem. Concr. Res.*, 2023, **174**, 107307.
32 R. K. Miao, N. Wang, S.-F. Hung, W.-Y. Huang, J. Zhang and Y. Zhao, *et al.*, Electrified Cement Production via Anion-Mediated Electrochemical Calcium Extraction, *ACS Energy Lett.*, 2023, **8**(11), 4694–4701.
33 T. Ji, S. Ren, Y. Yang, G. Jiang, G. V. Crescenzo and S. S. Scott, *et al.*, Low-emission cement clinker precursor production, enabled by electrolytic extraction of calcium from waste cement, *Nat. Commun.*, 2025, **16**(1), 9302.
34 R. J. Forster and J. P. O'Kelly, Protonation reactions of anthraquinone-2, 7-disulphonic acid in solution and within monolayers, *J. Electroanal. Chem.*, 2001, **498**(1–2), 127–135.
35 A. Tripodi, M. Compagnoni, G. Ramis and I. Rossetti, Pressure-swing or extraction-distillation for the recovery of pure acetonitrile from ethanol ammoxidation process: A comparison of efficiency and cost, *Chem. Eng. Res. Des.*, 2017, **127**, 92–102.
36 A. Ciaciuch and M. Sulewski, Recovery of the organic solvents from the multicomponent mixture in the process of the fractional distillation and the vacuum distillation, *Struct. Environ.*, 2024, **16**(2), 111–121.
37 A. Mezza, M. Bartoli, A. Chiodoni, J. Zeng, C. F. Pirri and A. Sacco, Optimizing the Performance of Low-Loaded Electrodes for CO_2-to-CO Conversion Directly from Capture Medium: A Comprehensive Parameter Analysis, *Nanomaterials*, 2023, **13**(16), 2314.
38 Z. Yan, L. Zhu, Y. C. Li, R. J. Wycisk, P. N. Pintauro and M. A. Hickner, *et al.*, The balance of electric field and interfacial catalysis in promoting water dissociation in bipolar membranes, *Energy Environ. Sci.*, 2018, **11**(8), 2235–2245.
39 *Understanding Water Dissociation in Bipolar Membranes for Applications in CO_2 Electrolyzers, ed. L. Chen, Q. Xu, K. Fabrizio and S. W. Boettcher,* The Electrochemical Society, Inc, 2023.
40 E. W. Lees, M. Goldman, A. G. Fink, D. J. Dvorak, D. A. Salvatore and Z. Zhang, *et al.*, Electrodes designed for converting bicarbonate into CO, *ACS Energy Lett.*, 2020, **5**(7), 2165–2173.
41 M. Igawa, K. Echizenya, T. Hayashita and M. Seno, Neutralization dialysis for deionization, *Bull. Chem. Soc. Jpn.*, 1987, **60**(1), 381–383.
42 A. Alok, R. Shrestha, S. Ban, S. Devkota, B. Uprety and R. Joshi, Technological advances in the transformative utilization of CO_2 to value-added products, *J. Environ. Chem. Eng.*, 2022, **10**(1), 106922.
43 L. Chen, Q. Xu, S. Z. Oener, K. Fabrizio and S. W. Boettcher, Design principles for water dissociation catalysts in high-performance bipolar membranes, *Nat. Commun.*, 2022, **13**(1), 3846.
44 K. Wedege, E. Dražević, D. Konya and A. Bentien, Organic redox species in aqueous flow batteries: redox potentials, chemical stability and solubility, *Sci. Rep.*, 2016, **6**(1), 39101.
45 C. Tang and M. L. Bruening, Ion separations with membranes, *J. Polym. Sci.*, 2020, **58**(20), 2831–2856.
46 G. Glenk, R. Meier and S. Reichelstein, Cost dynamics of clean energy technologies, *Schmalenbach J. Bus. Res.*, 2021, **73**(2), 179–206.

47 Electrolyzer cost projections compared to actual market costs: A Critical Analysis, in *2023 IEEE PES Innovative Smart Grid Technologies - Asia (ISGT Asia)*, ed. H. V. Ghadim, R. Canessa, J. Haas and R. Peer, 2023.
48 X. Liu, K. Jin, X. Li and R. Yang, Low-carbon cement manufacturing enabled by electrified calcium looping and thermal energy storage, *Int. J. Greenhouse Gas Control*, 2023, **129**, 103986.
49 S. A. Miller, G. Habert, R. J. Myers and J. T. Harvey, Achieving net zero greenhouse gas emissions in the cement industry via value chain mitigation strategies, *One Earth*, 2021, **4**(10), 1398–1411.
50 *Combined calcination and CO_2 capture in cement clinker production by use of electrical energy, ed. L.-A. Tokheim, A. Mathisen, L. E. Øi, C. K. Jayarathna, N. H. Eldrup and T. Gautestad, 2019.*
51 O. Oguntola and S. Simske, Continuous assessment of the environmental impact and economic viability of decarbonization improvements in cement production, *Resources*, 2023, **12**(8), 95.
52 A. Franco and M. Rocca, Renewable electricity and green hydrogen integration for decarbonization of ''hard-to-abate'' industrial sectors, *Electricity*, 2024, **5**(3), 471–490.
53 T. Hills, D. Leeson, N. Florin and P. Fennell, Carbon capture in the cement industry: technologies, progress, and retrofitting, *Environ. Sci. Technol.*, 2016, **50**(1), 368–377.
54 E. McNamee, Propelling the Commercialization of 'Novel Cements': An investigation of demand-side factors to accelerate decarbonizing technologies within the cement industry, IIIEE Master Thesis, 2020.
55 M. Schneider, V. Hoenig, J. Ruppert and J. Rickert, The cement plant of tomorrow, *Cem. Concr. Res.*, 2023, **173**, 107290.
56 V. J. Reddy, N. P. Hariram, M. F. Ghazali and S. Kumarasamy, Pathway to sustainability: An overview of renewable energy integration in building systems, *Sustainability*, 2024, **16**(2), 638.
57 D. J. D. Pimlott, Y. Kim and C. P. Berlinguette, Reactive carbon capture enables CO_2 electrolysis with liquid feedstocks, *Acc. Chem. Res.*, 2024, **57**(7), 1007–1018.
58 H. Song, C. A. Fernández, H. Choi, P.-W. Huang, J. Oh and M. C. Hatzell, Integrated carbon capture and CO production from bicarbonates through bipolar membrane electrolysis, *Energy Environ. Sci.*, 2024, **17**(10), 3570–3579.
59 M. Namdari, Y. Kim, D. J. D. Pimlott, A. M. L. Jewlal and C. P. Berlinguette, Reactive carbon capture using electrochemical reactors, *Chem. Soc. Rev.*, 2025, **54**(2), 590–600.
60 C. P. O'Brien, R. K. Miao, A. Shayesteh Zeraati, G. Lee, E. H. Sargent and D. Sinton, CO_2 Electrolyzers, *Chem. Rev.*, 2024, **124**(7), 3648–3693.
61 T. Li, E. W. Lees, M. Goldman, D. A. Salvatore, D. M. Weekes and C. P. Berlinguette, Electrolytic conversion of bicarbonate into CO in a flow cell, *Joule*, 2019, **3**(6), 1487–1497.
62 D. A. Salvatore, D. M. Weekes, J. He, K. E. Dettelbach, Y. C. Li and T. E. Mallouk, *et al.*, Electrolysis of Gaseous CO_2 to CO in a Flow Cell with a Bipolar Membrane, *ACS Energy Lett.*, 2017, **3**(1), 149–154.
63 B. Endrődi, A. Samu, E. Kecsenovity, T. Halmágyi, D. Sebők and C. Janáky, Operando cathode activation with alkali metal cations for high current density operation of water-fed zero-gap carbon dioxide electrolysers, *Nat. Energy*, 2021, **6**(4), 439–448.
64 D. M. Weekes, D. A. Salvatore, A. Reyes, A. Huang and C. P. Berlinguette, Electrolytic CO_2 reduction in a flow cell, *Acc. Chem. Res.*, 2018, **51**(4), 910–918.
65 Y. Kim, E. W. Lees, C. Donde, A. M. L. Jewlal, C. E. B. Waizenegger and B. M. W. de Hepcée, *et al.*, Integrated CO_2 capture and conversion to form syngas, *Joule*, 2024, **8**(11), 3106–3125.
66 T. Li, E. W. Lees, Z. Zhang and C. P. Berlinguette, Conversion of bicarbonate to formate in an electrochemical flow reactor, *ACS Energy Lett.*, 2020, **5**(8), 2624–2630.
67 E. W. Lees, A. Liu, J. C. Bui, S. Ren, A. Z. Weber and C. P. Berlinguette, Electrolytic methane production from reactive carbon solutions, *ACS Energy Lett.*, 2022, **7**(5), 1712–1718.
68 S. Ma, Y. Kim, Z. Zhang, S. Ren, C. Donde and L. Melo, *et al.*, Cathode surface pH modulates multicarbon product selectivity during the electrochemical conversion of CO_2 capture solutions, *ACS Energy Lett.*, 2024, **9**(5), 2326–2332.
69 Y. Kim, E. W. Lees and C. P. Berlinguette, Permeability matters when reducing CO_2 in an electrochemical flow cell, *ACS Energy Lett.*, 2022, **7**(7), 2382–2387.
70 Y. Xu, J. P. Edwards, J. Zhong, C. P. O'Brien, C. M. Gabardo and C. McCallum, *et al.*, Oxygen-tolerant electroproduction of C2 products from simulated flue gas, *Energy Environ. Sci.*, 2020, **13**(2), 554–561.
71 W. Luc, B. H. Ko, S. Kattel, S. Li, D. Su and J. G. Chen, *et al.*, SO_2-induced selectivity change in CO_2 electroreduction, *J. Am. Chem. Soc.*, 2019, **141**(25), 9902–9909.
72 B. H. Ko, B. Hasa, H. Shin, E. Jeng, S. Overa and W. Chen, *et al.*, The impact of nitrogen oxides on electrochemical carbon dioxide reduction, *Nat. Commun.*, 2020, **11**(1), 5856.
73 D. J. D. Pimlott, A. Jewlal, B. A. W. Mowbray and C. P. Berlinguette, Impurity-resistant CO_2 reduction using reactive carbon solutions, *ACS Energy Lett.*, 2023, **8**(4), 1779–1784.
74 Concentrating Solar-Thermal Power Basics Washington, DC: U.S. Department of Energy; Available from: https://www.energy.gov/eere/solar/concentrating-solar-thermal-power-basics.